AMERICAN SOCIETY FOR MICROBIOLOGY | Journal of Bacteriology®

RESEARCH ARTICLE

# $Ca^{2+}$-Induced Two-Component System CvsSR Regulates the Type III Secretion System and the Extracytoplasmic Function Sigma Factor AlgU in *Pseudomonas syringae* pv. tomato DC3000

**Maxwell R. Fishman,[a] Johnson Zhang,[a] Philip A. Bronstein,[a,b]* Paul Stodghill,[b] Melanie J. Filiatrault[a,b]**

[a]School of Integrative Plant Science, Section of Plant Pathology and Plant-Microbe Biology, Cornell University, Ithaca, New York, USA

[b]Emerging Pests and Pathogens Research Unit, Robert W. Holley Center for Agriculture and Health, Agricultural Research Service, U.S. Department of Agriculture, Ithaca, New York, USA

**ABSTRACT** Two-component systems (TCSs) of bacteria regulate many different aspects of the bacterial life cycle, including pathogenesis. Most TCSs remain uncharacterized, with no information about the signal(s) or regulatory targets and/or role in bacterial pathogenesis. Here, we characterized a TCS in the plant-pathogenic bacterium *Pseudomonas syringae* pv. tomato DC3000 composed of the histidine kinase CvsS and the response regulator CvsR. CvsSR is necessary for virulence of *P. syringae* pv. tomato DC3000, since Δ*cvsS* and Δ*cvsR* strains produced fewer symptoms than the wild type (WT) and demonstrated reduced growth on multiple hosts. We discovered that expression of *cvsSR* is induced by $Ca^{2+}$ concentrations found in leaf apoplastic fluid. Thus, $Ca^{2+}$ can be added to the list of signals that promote pathogenesis of *P. syringae* pv. tomato DC3000 during host colonization. Through chromatin immunoprecipitation followed by next-generation sequencing (ChIP-seq) and global transcriptome analysis (RNA-seq), we discerned the CvsR regulon. CvsR directly activated expression of the type III secretion system regulators, *hrpR* and *hrpS*, that regulate *P. syringae* pv. tomato DC3000 virulence in a type III secretion system-dependent manner. CvsR also indirectly repressed transcription of the extracytoplasmic sigma factor *algU* and production of alginate. Phenotypic analysis determined that CvsSR inversely regulated biofilm formation, swarming motility, and cellulose production in a $Ca^{2+}$-dependent manner. Overall, our results show that CvsSR is a key regulatory hub critical for interaction with host plants.

**IMPORTANCE** Pathogenic bacteria must be able to react and respond to the surrounding environment, make use of available resources, and avert or counter host immune responses. Often, these abilities rely on two-component systems (TCSs) composed of interacting proteins that modulate gene expression. We identified a TCS in the plant-pathogenic bacterium *Pseudomonas syringae* that responds to the presence of calcium, which is an important signal during the plant defense response. We showed that when *P. syringae* is grown in the presence of calcium, this TCS regulates expression of factors contributing to disease. Overall, our results provide a better understanding of how bacterial pathogens respond to plant signals and control systems necessary for eliciting disease.

**KEYWORDS** *Pseudomonas syringae*, alginate, biofilms, calcium signaling, two-component regulatory systems

*Pseudomonas syringae* is a hemibiotrophic plant-pathogenic bacterial species composed of approximately 50 pathovars that differ in their host range (1, 2). This species causes significant economic losses to a number of crops, with certain pathovars being responsible for severe outbreaks of disease worldwide. Recent outbreaks include bleeding canker disease on horse chestnut caused by *P. syringae* pv. aesculi and

**Received** 7 September 2017 **Accepted** 12 December 2017

**Accepted manuscript posted online** 20 December 2017

**Citation** Fishman MR, Zhang J, Bronstein PA, Stodghill P, Filiatrault MJ. 2018. $Ca^{2+}$-induced two-component system CvsSR regulates the type III secretion system and the extracytoplasmic function sigma factor AlgU in *Pseudomonas syringae* pv. tomato DC3000. J Bacteriol 200:e00538-17. https://doi.org/10.1128/JB.00538-17.

**Editor** George O'Toole, Geisel School of Medicine at Dartmouth



Address correspondence to Melanie J. Filiatrault, Melanie.filiatrault@ars.usda.gov.

* Present address: Philip A. Bronstein, USDA-Food Safety Inspection Service, Washington, DC, USA.

bleeding canker disease on kiwi caused *P. syringae* pv. actinidiae (3, 4). *P. syringae* pv. tomato DC3000 causes bacterial speck of tomato and was one of the first bacterial plant pathogens to be sequenced (5). *P. syringae* pv. tomato DC3000 is frequently used for deciphering molecular plant-pathogen interactions due to its ability to infect both tomato and *Arabidopsis thaliana*. Research on *P. syringae* pv. tomato DC3000 has provided insights into the role of the type III secretion system (T3SS) in host-nonhost interactions and the role that type III effectors (T3Es) play in triggering the hypersensitive response (HR) in nonhosts (6). *P. syringae* pv. tomato DC3000 has a well-annotated genome, making it an ideal candidate for understanding the physiology of plant-pathogenic bacteria and understanding host-pathogen interactions.

*P. syringae* pv. tomato DC3000 requires a T3SS to deliver effectors into host cells and become pathogenic. Hypersensitive response and pathogenicity (*hrp*) genes and *hrp* conserved (*hrc*) genes code for the structural components of the T3SS, while *hrp* outer protein (*hop*) genes and avirulence (*avr*) genes code for the secreted T3Es (7, 8). Both T3SS and T3E genes are in turn regulated by a subset of *hrp* genes. The extracytoplasmic function (ECF) sigma factor HrpL directly regulates both *hrc* and *hop* genes (9, 10). The enhancer binding proteins (EBPs), HrpR and HrpS, form a heterohexameric complex that binds and activates $\sigma^{54}$ and allows for transcription of *hrpL* (11). In addition to regulating transcription of *hrpL*, HrpR and HrpS regulate transcription of many genes that are not in the HrpL regulon (12). No direct transcriptional activators have been described for *hrpR* and *hrpS*; however, the TCS RhpRS has been shown to be a direct repressor of *hrpR* and *hrpS* (13).

In *P. syringae* pv. tomato DC3000, multiple sensory systems regulate the T3SS and *hrp* genes, including GacA and AlgU (14, 15). The response regulator, GacA, regulates expression of the small RNAs (sRNAs) *rsmX*, *rsmY*, *rsmZ*, and five additional *rsmX* paralogs in *P. syringae* pv. tomato DC3000 (16). The *rsmZ* and *rsmY* sRNAs in turn bind and sequester the global regulator RsmA, while it is still unclear whether the *rsmX* sRNAs bind RsmA as well (14, 16). RsmA regulates a variety of genes posttranscriptionally in *P. syringae*, including genes that code for components of the T3SS, phytoxins, and pyoverdine (17). The ECF sigma factor AlgU has been primarily characterized as the regulator of production of the negatively charged exopolysaccharide (EPS) alginate in *Pseudomonas* (15, 18). In *P. syringae* pv. tomato DC3000, AlgU also regulates genes involved in osmotolerance, reactive oxygen species (ROS) tolerance, motility, and pathogenicity (15). In the case of pathogenicity, AlgU regulates *hrpR*, *hrpS*, and *hrpL* (15). Regulation of the T3SS through sensory systems highlights the importance of environmental signals during *P. syringae* pv. tomato DC3000 pathogenesis.

$Ca^{2+}$ is abundant in the apoplast, and little is known about its role as an environmental signal for *P. syringae* pv. tomato DC3000 (19). During a compatible interaction between *P. syringae* and the common bean, *Phaseolus vulgaris*, the concentration of $Ca^{2+}$ increases within the apoplast (20). Similar increases in $Ca^{2+}$ concentration occurs in the xylem of *Nicotiana tabacum* infected with *Xylella fastidiosa* (21). Bacteria strictly regulate $Ca^{2+}$ concentrations in the cytoplasm at a much lower concentration than $Ca^{2+}$ concentrations found extracellularly (22). This difference in concentration allows bacteria to use $Ca^{2+}$ as an environmental signal (22–24). Changes in extracellular $Ca^{2+}$ concentrations modulate several bacterial virulence traits for animal pathogens, including biofilm formation, motility, EPS production, T3SS deployment, and quorum sensing (25–32). Changes in $Ca^{2+}$ concentration also affect pectinolytic enzyme production in the necrotrophic plant pathogen *Pectobacterium carotovorum* and affect biofilm formation in the xylem-limited plant pathogen *Xylella fastidiosa* (32, 33). However, in many hemibiotrophic bacterial plant pathogens, such as *Pseudomonas syringae*, *Xanthomonas*, and *Ralstonia*, there is little known about how these pathogens respond to changes in $Ca^{2+}$ concentration and whether there are regulatory systems induced by $Ca^{2+}$. Given the abundance of $Ca^{2+}$ in the plant apoplast, it is possible that $Ca^{2+}$ represents an important signaling molecule for this group of plant pathogens.

Bacteria have evolved TCSs and ECF sigma factors to react to changes in the extracellular environment. TCSs transform signals perceived by bacteria into a cellular

response using a signal relay that is commonly made up of a transmembrane histidine kinase (HK) and an intracellular response regulator (RR). During signal transduction, an HK will typically transfer a phosphate group to an RR. Following phosphorylation, the RR will perform its designated function, such as binding DNA to regulate the expression of genes (34). The genome of *P. syringae* pv. tomato DC3000 encodes a large number of HKs and RRs (69 HKs and 95 RRs), many of which remain uncharacterized (35). We have previously reported that expression of a TCS in *P. syringae* pv. tomato DC3000 encoded by PSPTO_3380 (HK) and PSPTO_3381 (RR) is induced by $Fe^{3+}$ (36). The expression pattern is similar to the expression pattern of HrpL-regulated genes (36). However, PSPTO_3380 and PSPTO_3381 are not considered to be part of the HrpL regulon (9, 10). We also found that PSPTO_3380 and PSPTO_3381 are directly regulated by the ferric uptake regulator (37). In the current study, we showed that PSPTO_3380 and PSPTO_3381 represent a $Ca^{2+}$-induced, virulence-associated TCS in *P. syringae* pv. tomato DC3000. We also identified the PSPTO_3381 regulon using chromatin immunoprecipitation followed by next-generation sequencing (ChIP-seq) and transcriptome analysis (RNA-seq). In reference to the phenotype of PSPTO_3380 and PSPTO_3381, we suggest naming this TCS the calcium, virulence, and swarming sensor (CvsS) and regulator (CvsR) and refer to it as such throughout this article.

## RESULTS

**CvsS and CvsR affect virulence of *P. syringae* pv. tomato DC3000.** In order to determine if *cvsS* and *cvsR* affect the ability of *P. syringae* pv. tomato DC3000 to cause disease, tomato plants were dip inoculated with Δ*cvsS* and Δ*cvsR P. syringae* pv. tomato DC3000 strains. At 6 days postinoculation (dpi), tomato plants inoculated with either the Δ*cvsS* or Δ*cvsR* strain produced fewer symptoms than those inoculated with the wild-type (WT) strain (Fig. 1A). The Δ*cvsS* and Δ*cvsR* strains also showed reduced growth on tomato plants compared to the WT at 4 dpi and 6 dpi (Fig. 1B). Both symptoms and growth of the Δ*cvsR* strain could be partially restored with a single-copy chromosomal complementation of *cvsR* (*cvsR*c) (Fig. 1A and B). In addition, *A. thaliana* was vacuum infiltrated with either the WT, Δ*cvsS*, or Δ*cvsR P. syringae* pv. tomato DC3000 strain to determine whether CvsSR was involved in virulence for multiple hosts. Similar to the case for tomato plants, *A. thaliana* plants inoculated with the Δ*cvsS* and Δ*cvsR* strains showed a reduction in symptom development as well as a reduction in growth compared to those inoculated with the WT (Fig. 1C and D). These results demonstrate that CvsSR is associated with growth and virulence of *P. syringae* pv. tomato DC3000 in multiple hosts. In addition, since reduced virulence was observed upon dip inoculation (a natural mode of entry via stomates) and vacuum infiltration (which bypasses natural entry), we conclude that CvsSR is necessary for full virulence of *P. syringae* pv. tomato DC3000 during growth in the apoplast.

**Calcium induces expression of *cvsSR*.** The TCS orthologous to CvsSR in *Pseudomonas aeruginosa* is induced by $Ca^{2+}$ (38). To test for induction of *cvsS* and *cvsR* by $Ca^{2+}$, we designed a luciferase promoter gene construct that included 400 bp upstream of PSPTO_3383 ($P_{cvsSR}$), which included a previously mapped transcriptional start site for PSPTO_3383, and introduced it into WT, Δ*cvsS*, and Δ*cvsR* strains of *P. syringae* pv. tomato DC3000 (39). Expression of this construct should reflect expression of the promoter for *cvsS* and *cvsR*, as we found that *cvsS*, *cvsR*, PSPTO_3382, and PSPTO_3383 formed an operon by using reverse transcription-PCR (RT-PCR) (see Fig. S1 in the supplemental material). The addition of $Ca^{2+}$ to mannitol glutamate (MG) medium resulted in a significant increase in $P_{cvsSR}$ after 6 h of growth compared to the basal level of expression in MG medium (Fig. 2A). To test whether the chelation of $Ca^{2+}$ would inhibit $Ca^{2+}$-induced expression of $P_{cvsSR}$, we added the $Ca^{2+}$ chelator EGTA to MG medium supplemented with $Ca^{2+}$. No increase in expression of $P_{cvsSR}$ was observed when *P. syringae* pv. tomato DC3000 was grown in MG medium supplemented with $Ca^{2+}$ and EGTA compared to when *P. syringae* pv. tomato DC3000 was grown in MG medium (Fig. 2A). From these data, we conclude that expression of $P_{cvsSR}$ is induced by $Ca^{2+}$.

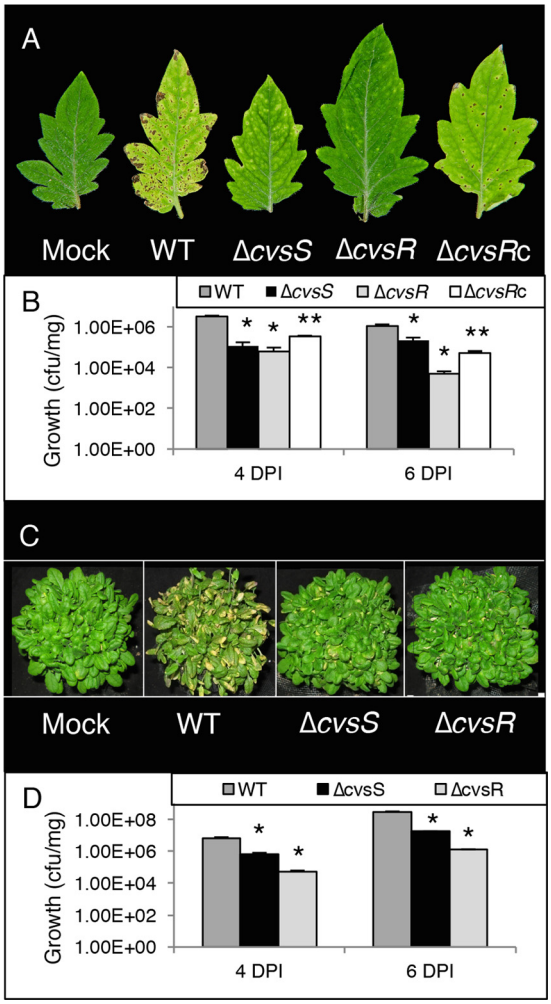


**FIG 1** Growth and symptoms of WT, Δ*cvsS*, and Δ*cvsR* strains on tomato and *A. thaliana*. (A) Image of symptoms at 6 dpi of tomato dip inoculated with *P. syringae* pv. tomato DC3000 strains. (B) Growth (CFU/mg) at 4 dpi and 6 dpi for the WT, Δ*cvsS*, Δ*cvsR*, and Δ*cvsR*c strains infecting tomato. The strains were inoculated at $2 \times 10^7$ CFU/ml. Average bacterial growth in three plants is shown, with the error bars representing the standard error between the three replicates. (C) Image of symptoms at 4 dpi on *A. thaliana* vacuum infiltrated with *P. syringae* pv. tomato DC3000 strains. (D) Growth (CFU/mg) at 4 dpi and 6 dpi for the WT, Δ*cvsS*, and Δ*cvsR* strains infecting *A. thaliana* that had been inoculated at $3 \times 10^4$ CFU/ml. Average bacterial growth in three plants is shown, with the error bars representing the standard error between the three replicates. In panels B and D, * denotes a statistically significant difference with a *P* value of $<0.01$ between growth of the WT and Δ*cvsS* and Δ*cvsR* strains and ** denotes a statistically significant difference with a *P* value of $<0.01$ between the Δ*cvsR* and Δ*cvsR*c strains, determined using Student's two-tailed *t* test.

TCSs, including the TCS orthologous to CvsSR in *P. aeruginosa*, commonly autoregulate (40). We compared the expression of $P_{cvsSR}$ in the Δ*cvsS* and Δ*cvsR* strains to that in the WT when grown in MG medium supplemented with $Ca^{2+}$. Expression of $P_{cvsSR}$ was significantly reduced in the Δ*cvsS* and Δ*cvsR* strains compared to the WT (Fig. 2B). These data show that CvsSR positively autoregulates.

The leaf apoplast contains anywhere from 10 $\mu$M to 10 mM free $Ca^{2+}$ (19). Based on these data, we hypothesized that $Ca^{2+}$ could induce expression of *cvsSR* during growth *in planta*. Apoplastic washing fluid (AWF) was extracted from tomato leaves, and elemental analysis was then performed using inductively coupled plasma-mass spectroscopy (ICP-MS). Based on data from three samples, the concentration of calcium in the tomato leaf apoplast was an average of 9.7 mM with a standard deviation of 0.1 mM (see Table S1 in the supplemental material). Therefore, we concluded that the concentration of $Ca^{2+}$ was likely high enough to induce expression of $P_{cvsSR}$ in AWF. We grew

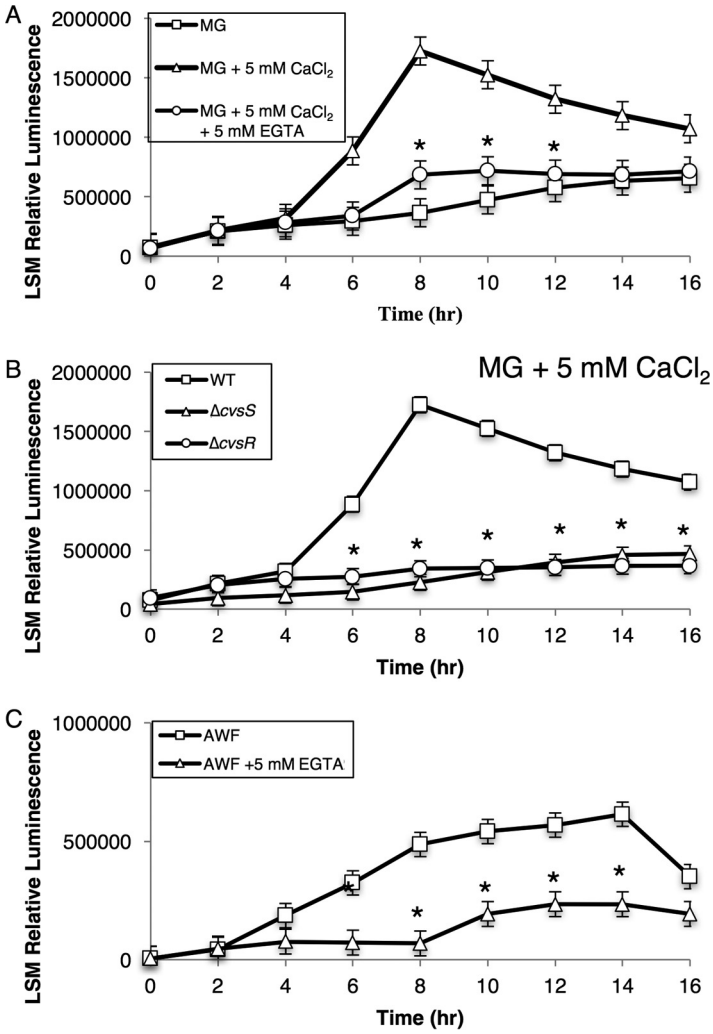


**FIG 2** Luminescence assays to assess activity of $P_{cvsSR}$ in the WT grown in MG, MG with 5 mM $CaCl_2$, and MG with 5 mM $CaCl_2$ and 5 mM EGTA over the course of 16 h (A), in the WT, Δ*cvsS*, and Δ*cvsR* strains grown in MG with 5 mM $CaCl_2$ (B), and in the WT grown in AWF and AWF with 5 mM EGTA (C). The relative luminescence was calculated by using the total luminescence relative to $OD_{600}$. Experiments were performed three times. The three experiments were compiled using a least-squares mean regression. The error bars represent standard deviation generated by the differences observed between samples. * denotes statistically significant differences determined using a Tukey honestly significant difference (HSD) test with a *P* value of $<0.01$ between MG with 5 mM $CaCl_2$ and the two other conditions (A), between the WT and Δ*cvsS* and Δ*cvsR* strains (B), and between AWF and AWF with 5 mM EGTA (C).

*P. syringae* pv. tomato DC3000 in AWF and found that $P_{cvsSR}$ increased over time (Fig. 2C). Addition of EGTA to AWF reduced expression of $P_{cvsSR}$, suggesting that $Ca^{2+}$ likely induced *cvsSR* in AWF and also *in planta* (Fig. 2C).

**Identification of direct targets for CvsR in *P. syringae* pv. tomato DC3000.** ChIP-seq was employed in order to determine regions of the genome bound by the predicted DNA binding response regulator CvsR. The Δ*cvsR P. syringae* pv. tomato DC3000 strain was complemented with pBS46::*cvsR*-FLAG (Δ*cvsR cvsR*-FLAG). To determine if the FLAG-tagged protein was active, expression of pBS59::$P_{cvsSR}$ was evaluated in the Δ*cvsR cvsR*-FLAG strain. When the Δ*cvsR cvsR*-FLAG strain was grown in MG medium supplemented with $Ca^{2+}$, expression of $P_{cvsSR}$ was induced (see Fig. S2 in the supplemental material), suggesting that CvsR-FLAG was active. The Δ*cvsR cvsR*-FLAG strain was then grown for 18 h on nutrient broth (NB) agar plates supplemented with $Ca^{2+}$ and succinate before cells were collected for ChIP. Prior to sequencing, the genomic region upstream of PSPTO_3383 and *gyrA* were used as positive and negative

controls, respectively, to determine enrichment of the immunoprecipitation (IP) fraction compared to the input fraction. The genomic region upstream of PSPTO_3383 was chosen as a positive control because CvsSR positively autoregulates and likely binds to an area near the previously mapped transcriptional start site for the operon that includes PSPTO_3383 (39). The gene *gyrA* had been used as a negative control in a previous ChIP-seq experiment on *P. syringae* pv. tomato DC3000 (37). It was determined that the region upstream of PSPTO_3383 was enriched 6.4-fold in the IP fraction compared to the input fraction, while no enrichment was observed for *gyrA* in the IP fraction compared to the input fraction. Sequencing was performed on libraries made from the IP and input samples. Overall, 5,609,692 reads were sequenced from the IP sample and 1,366,470 reads were sequenced from the input sample. In both cases, 97% of the reads aligned to the *P. syringae* pv. tomato DC3000 genome. Using MACS2, 199 peaks were identified using a false-discovery rate (FDR) cutoff of less than 0.05 (see Data Set S1 in the supplemental material). Enriched peaks were found upstream of the gene PSPTO_5255, which codes for a carbonic anhydrase, and within the gene PSPTO_4969, which codes for an RHS repeat protein (Fig. 3A). Of note, two peaks were found upstream of the global virulence regulator *hrpR* (Fig. 3A). This makes CvsR the second described direct transcriptional regulator or *hrpR* (13). The first peak was found 749 bp upstream of the translational start site for *hrpR* (peak 1), and the second peak was found 63 bp upstream of the translational start site for *hrpR* (peak 2). No peak was called in the area upstream of PSPTO_3383. This was due to the fact that the area was disregarded during the peak calling using MACS because there was a large peak in *cvsR* due to the overexpression of this gene.

Ten areas of the genome that showed enrichment in the ChIP-seq data were selected for further evaluation by electrophoretic mobility shift assays (EMSA) and DNase footprinting to confirm binding by CvsR. The 10 areas investigated included the genomic regions upstream of PSPTO_5255, PSPTO_0203, *katB*, *oprF*, *hrpR*, *gidA*, *t-RNA*, *cys-1*, and *spf* and within the gene PSPTO_4969 (Fig. 3B and C; see Fig. S3, S4, and S5 in the supplemental material). The area upstream of the gene PSPTO_0786 was used as a negative control for CvsR binding (Fig. S3 and S4). All showed a binding site by using DNase footprinting, and all of these areas except for the area upstream of *oprF* showed a clear shift by EMSA. It is possible that CvsR did not have a high affinity for the area of the genome upstream of *oprF* and that this was reflected in the undefined gel shift. It should be noted that according to the EMSA, CvsR showed a higher binding affinity for the peak 749 bp upstream of the translational start site for *hrpR* than for the second peak 63 bp upstream of the translational start site for *hrpR*.

We also checked for binding of CvsR upstream of PSPTO_3383 since CvsSR autoregulates and the operon includes *cvsS* and *cvsR*. The probe we created upstream of PSPTO_3383 included the putative transcriptional start site for the operon (39). We found that CvsR bound upstream of PSPTO_3383 (Fig. S3 and S4). These data provide additional support that CvsR autoregulates.

Using the 199 peaks we identified above, one 10-nucleotide (nt)-long binding motif for CvsR was determined (Fig. 3D). This type of motif is common for RRs in the OmpR family and suggests that only a single motif is required for CvsR to bind DNA (41). DNase footprinting data were consistent with this prediction, since binding sites mapped for *hrpR* peak 2 and PSPTO_0203 were approximately 11 to 14 bp and covered a single predicted binding motif (Fig. S5). Other areas from the DNase footprinting, like those mapped for PSPTO_5255 and *hrpR* peak 1, spanned around 26 bp and covered two direct repeats similar to the predicted binding motif (Fig. S5). A predicted binding motif was also produced using all the sites CvsR bound that were identified using the DNase footprinting probes (see Fig. S6 in the supplemental material). The resulting motif was similar to the one determined from the ChIP-seq data.

**Mapping the transcriptional landscape of CvsR.** RNA-seq was used to complement the ChIP-seq data and more thoroughly determine the CvsR regulon. The same condition used to grow cells for the ChIP-seq analysis was also used for extracting RNA

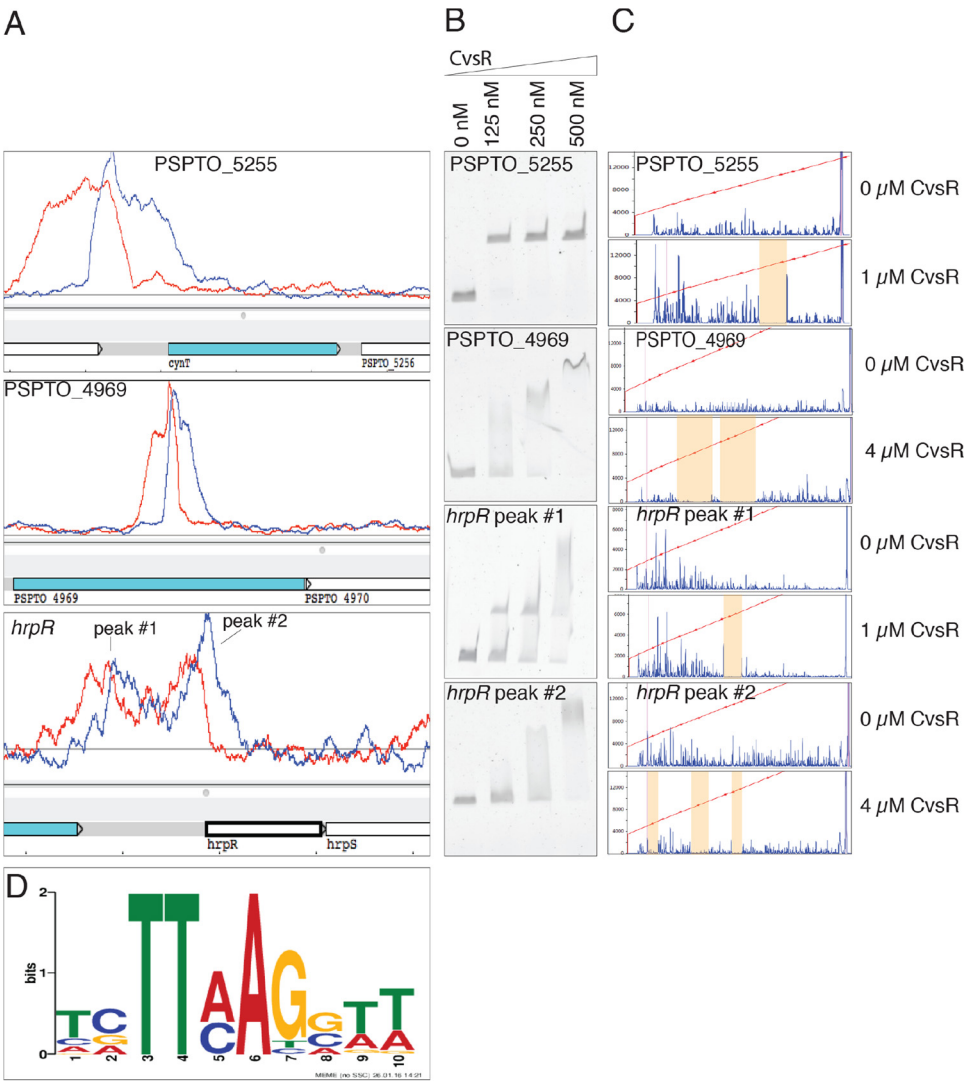


**FIG 3** Visualization of ChIP-seq data, CvsR DNA binding assays, and a putative CvsR binding motif. (A) Screenshot of the Artemis genome browser depicting areas of enrichment (peaks) in the ChIP-seq data upstream of PSPTO_5255, within PSPTO_4969, and upstream of *hrpR*. The red line represents the forward strand of DNA, while the blue line represents the reverse strand of DNA. ChIP-seq peaks occur where enriched areas for each strand overlap. (B) EMSA with concentrations of CvsR increasing from left to right for probes that code for genomic locations found within the ChIP-seq peaks for PSPTO_5255, PSPTO_4969, and *hrpR*. A shift in the migration of the probe with increasing concentrations of CvsR signifies binding of CvsR to that probe. (C) Fluorescent, nonradioactive DNase footprinting assays showing binding of CvsSR. The red line is a line of best fit that estimates the size (in base pairs) of each fragment made using a LIZ500 ladder. The blue peaks are fluorescent signal and represent the size of fragmented DNA. The areas that are highlighted in orange are regions with little fluorescence when CvsR is added at 1 $\mu$M or 4 $\mu$M to the reaction mixture compared to when no CvsR is added. These regions signify areas in the probes that were bound by CvsR. (D) Predicted binding motif for CvsR that was compiled by MEME using the areas 50 bp upstream and 50 bp downstream of the center of the ChIP-seq peak.

for RNA-seq analysis. On average, 50,421,230 reads were generated from the Δ*cvsR* strain cDNA libraries and 35,215,281 reads were generated for the WT cDNA libraries. Of those reads, 97% aligned to the *P. syringae* pv. tomato DC3000 genome. From these data sets, 292 genes were differentially regulated between the WT and the Δ*cvsR* strain by 2-fold or more using an FDR cutoff less than 0.05. Of these genes, 181 genes were upregulated and 111 genes were downregulated in the Δ*cvsR* strain compared to the WT (see Data Set S2 in the supplemental material). A subset of these genes is listed in Table 1. Changes in expression of a subset of differentially expressed genes were confirmed using qRT-PCR (see Data Set S3 in the supplemental material). Within the

**TABLE 1** Selected genes differentially expressed between WT and Δ*cvsR* strains

| Category | Locus no[a] | Gene[b] | Description[c] | Fold change[d] |
|---|---|---|---|---|
| Motility | PSPTO_0911 | *cheW* | Chemotaxis protein | −2.24 |
| | PSPTO_0915 | *cheY* | Chemotaxis protein | −2.73 |
| | PSPTO_1933 | *flgB* | Flagellar basal body rod protein | −2.55 |
| | PSPTO_1936 | *flgE* | Flagellar hook protein | −2.55 |
| | PSPTO_1949 | *fliC* | Flagellin | −4.51 |
| | PSPTO_1952 | *fliS* | Flagellar protein | −2.20 |
| | PSPTO_1953 | *flgD* | Basal body rod modification protein | −2.35 |
| | PSPTO_4156 | *motY* | Sodium-type flagellar protein | −2.13 |
| Alginate biosynthesis and regulation | PSPTO_1232 | *algA* | Alginate biosynthesis protein | 2.81 |
| | PSPTO_1233 | *algF* | Alginate biosynthesis protein | 3.01 |
| | PSPTO_1234 | *algJ* | Probable alginate *O*-acetylase | 3.21 |
| | PSPTO_1235 | *algI* | Probable alginate *O*-acetylase | 2.42 |
| | PSPTO_1236 | *algL* | Alginate lyase | 2.68 |
| | PSPTO_1237 | *algX* | Alginate biosynthesis protein | 2.86 |
| | PSPTO_1238 | *algG* | Poly(beta-D-mannuronate) C-5 epimerase | 3.27 |
| | PSPTO_1239 | *algE* | Alginate production protein | 3.29 |
| | PSPTO_1240 | *algK* | Alginate biosynthesis protein | 3.60 |
| | PSPTO_1241 | *alg44* | Alginate biosynthesis protein | 3.15 |
| | PSPTO_1243 | *algD* | GDP-mannose 6-dehydrogenase | 2.56 |
| | PSPTO_4222 | *algU* | RNA polymerase sigma factor | 2.64 |
| | PSPTO_4222 | *mucB* | Sigma factor *algU* regulatory protein | 2.46 |
| | PSPTO_4223 | *mucA* | Sigma factor *algU* negative regulatory protein | 2.19 |
| *rsm* sRNA | PSPTO_5647 | *rsmY* | sRNA | −3.12 |
| | PSPTO_5671 | *rsmX* | sRNA | −2.23 |
| | PSPTO_5673 | *rsmX-3* | sRNA | −8.02 |
| | PSPTO_5674 | *rsmX-4* | sRNA | −3.54 |
| Sulfur uptake and regeneration | PSPTO_0203 | | Cysteine synthase | −2.04 |
| | PSPTO_0308 | *sbp* | Sulfate binding protein | 8.20 |
| | PSPTO_0309 | *cysT* | Sulfate ABC transporter | 2.73 |
| | PSPTO_0310 | | Sulfate ABC transporter | 3.13 |
| | PSPTO_0311 | *cysA* | Sulfate/thiosulfate import ATP binding protein | 3.21 |
| | PSPTO_1793 | | Uncharacterized protein | 2.83 |
| | PSPTO_1795 | | Alkanesulfonate monooxygenase | 2.41 |
| | PSPTO_1796 | | Sulfonate ABC transporter | 2.43 |
| | PSPTO_1797 | | Aliphatic sulfonates import ATP binding protein | 2.27 |
| | PSPTO_2614 | | Dioxygenase, TauD/TfdA family | 2.31 |
| | PSPTO_3438 | *iscS-3* | Cysteine desulfurase | 3.53 |
| | PSPTO_3451 | *ssuE* | Flavin mononucleotide reductase, NADH dependent | 34.00 |
| | PSPTO_3466 | *ssuD* | Alkanesulfonate monooxygenase | 15.76 |
| | PSPTO_4161 | | Glutaredoxin | −2.04 |
| | PSPTO_5187 | *metQ-1* | D-Methionine binding lipoprotein | 12.99 |
| | PSPTO_5188 | *metN-1* | Methionine import ATP binding protein | 7.68 |
| | PSPTO_5189 | *metI-1* | D-Methionine ABC transporter | 5.76 |
| | PSPTO_5198 | | Dioxygenase, TauD/TfdA family | 11.10 |
| | PSPTO_5312 | *tauC* | Taurine ABC transporter | 3.29 |
| | PSPTO_5314 | | Aliphatic sulfonate import ATP binding protein | 17.20 |
| | PSPTO_5315 | *ssuC* | Aliphatic sulfonate ABC transporter | 18.16 |
| | PSPTO_5316 | | Sulfonate ABC transporter | 16.76 |
| | PSPTO_5319 | *tauA* | Taurine ABC transporter | 3.74 |
| | PSPTO_5320 | *tauB* | Taurine import ATP binding protein | 3.02 |
| Quorum sensing | PSPTO_2048 | | Transcriptional regulator, LuxR family | −4.12 |
| | PSPTO_2590 | | Bacterial luciferase family protein | −4.12 |
| | PSPTO_5548 | | DNA binding response regulator, LuxR family | −11.62 |

[a]Locus number of differentially expressed gene.
[b]Gene name of differentially expressed gene (if applicable).
[c]Putative functional description of gene product or sRNA as listed in the InterPro database (96).
[d]Fold change of gene expression between the Δ*cvsR* strain and the WT according to RNA-seq data.

RNA-seq data set, ChIP-seq peaks were found within or upstream of 19 genes that were also differentially expressed in the Δ*cvsR* strain. These genes are listed in Table 2.

**CvsSR regulates expression of *algU*.** RNA-seq results showed a greater-than-2-fold increase in expression of *algU*, *mucA*, and *mucB* in the Δ*cvsR* strain. In addition, 94 genes

**TABLE 2** Genes in the CvsR primary regulon

| Nearest gene ID[a] | Gene name[b] | Description[c] | Fold change[d] |
|---|---|---|---|
| PSPTO_0203 | | Cysteine synthase | −2.04 |
| PSPTO_0279 | | Uncharacterized protein | −2.62 |
| PSPTO_1062 | | Uncharacterized protein | −2.52 |
| PSPTO_1304 | | Uncharacterized protein | −6.23 |
| PSPTO_1609 | | Uncharacterized protein | −3.10 |
| PSPTO_1626 | | Uncharacterized protein | 2.11 |
| PSPTO_2809 | | Uncharacterized protein | 2.10 |
| PSPTO_3086 | | Transcriptional regulator | 11.29 |
| PSPTO_3288 | | Uncharacterized protein | 6.13 |
| PSPTO_3289 | | Uncharacterized protein | 3.83 |
| PSPTO_3318 | | Beta-glucosidase | 2.53 |
| PSPTO_3582 | *katB* | Catalase | 2.86 |
| PSPTO_4631 | | Sensory box/GGDEF domain/EAL domain protein | −3.07 |
| PSPTO_5255 | *cynT* | Carbonic anhydrase | −23.64 |
| PSPTO_5256 | | Sulfate transporter family protein | −9.02 |
| PSPTO_5312 | | Conserved domain protein | 3.78 |
| PSPTO_5316 | | Sulfonate ABC transporter | 16.76 |
| PSPTO_5319 | *tauA* | Taurine ABC transporter | 3.74 |
| PSPTO_5466 | | Uncharacterized protein | −2.71 |
| PSPTO_t37 | tRNA-Cys-1 gene | tRNA-Cys-1 | −2.21 |

[a]Nearest gene ID downstream of a ChIP-seq peak.
[b]If applicable.
[c]Putative functional description of gene product as listed in the UniProt database (97).
[d]Fold change of gene expression between the Δ*cvsR* strain and the WT according to RNA-seq data.

previously reported to be part of the AlgU regulon are shared with the CvsR regulon (15). Of these 94 genes, 77 displayed the same expression profile in an *algU*-overexpressing strain and in the Δ*cvsR* strain compared to the WT. Notably, genes involved in alginate production, including *algD*, showed increased expression in the Δ*cvsR* strain compared to the WT. The Δ*cvsS* and Δ*cvsR* strains grown on NB agar supplemented with $Ca^{2+}$ showed a significant increase in alginate production after 12 h of growth compared to the WT but not when grown on NB agar (Fig. 4A; see Fig. S7 in the supplemental material). This provides additional confirmation that CvsSR regulates expression of genes involved in alginate production and that AlgU is active in the Δ*cvsS* and Δ*cvsR* strains. Since deletion of *cvsR* resulted in increased *algU* expression compared to the WT and CvsS and CvsR regulate alginate production, we conclude that CvsSR indirectly regulates expression of *algU* in *P. syringae* pv. tomato DC3000.

**CvsSR regulates bacterial cell attachment and motility.** Expression of genes involved in flagellar motility decreased in the Δ*cvsR* strain compared to the WT, and several genes involved in quorum sensing were also differentially expressed in the Δ*cvsR* strain compared to the WT (Table 1). In *Pseudomonas*, biofilm formation and swarming motility can be impacted by changes in alginate production, flagellar biosynthesis, and quorum-sensing genes (42–44). Biofilm assays were performed in MG medium supplemented with $Ca^{2+}$. The Δ*cvsR* strain, but not the Δ*cvsS* strain, showed a significant increase in attachment compared to the WT (Fig. 4B). Swarming motility of the Δ*cvsS* and Δ*cvsR* strains was reduced compared to the that of WT when $Ca^{2+}$ was added to swarming medium but not on standard swarming medium (Fig. 4C and D; see Fig. S8 in the supplemental material). This phenotype was partially complemented in the Δ*cvsR*c strain (Fig. 4C and D). It should be noted that the Δ*cvsR*c strain was unable to swarm as well as the WT on swarming medium and on swarming medium supplemented with $Ca^{2+}$ (Fig. 4D and S8). Swimming assays were performed to determine whether the Δ*cvsS* and Δ*cvsR* strains had decreased flagellar motility compared to the WT and whether decreased flagellar motility explained the decreased swarming in the Δ*cvsS* and Δ*cvsR* strains. No difference in swimming motility was found between the Δ*cvsS* and Δ*cvsR* strains and the WT, suggesting that the decreased swarming motility exhibited by the Δ*cvsS* and Δ*cvsR* strains was likely not due to decreased flagellar

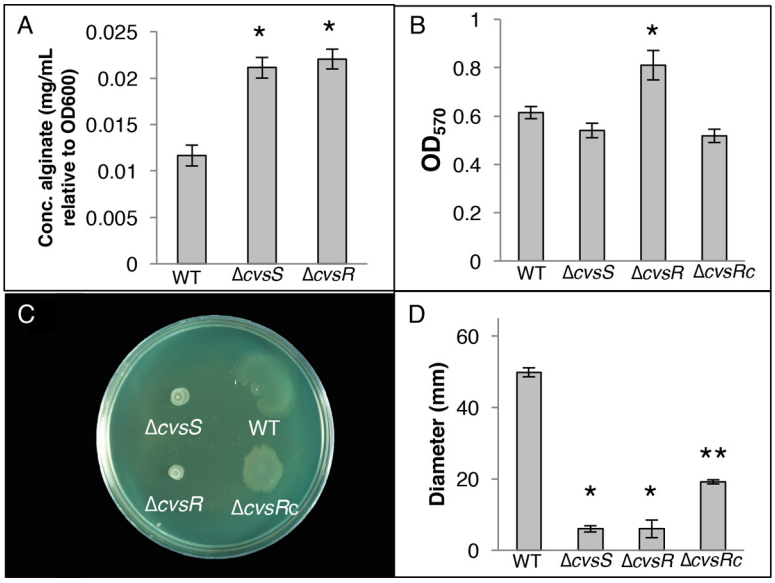


**FIG 4** Assays assessing phenotypic changes in the Δ*cvsS* and Δ*cvsR* strains compared to the WT. (A) Amount of alginate present in the WT, Δ*cvsS*, and Δ*cvsR* strains of *P. syringae* pv. tomato DC3000 when grown on NB agar supplemented with 5 mM $CaCl_2$ for 12 h. This assay was performed three times. * denotes a statistically significant difference with a *P* value of $<0.01$ between the WT and the Δ*cvsS* and Δ*cvsR* strains, was determined using Student's two-tailed *t* test. (B) Biofilm formation by the WT, Δ*cvsS*, Δ*cvsR*, and Δ*cvsR*c strains grown in MG (pH 7.0) with 2 mM $CaCl_2$ visualized using absorbance of crystal violet at 570 nm. The error bars represent the standard deviation between the replicates. This assay was repeated three times. * denotes a statistically significant difference with a *P* value of $<0.05$ between the WT and the Δ*cvsR* strain, determining using Student's two-tailed *t* test. (C) Swarming assays of the WT, Δ*cvsS*, Δ*cvsR*, *and* Δ*cvsR*c strains grown on medium with 5 mM $CaCl_2$. Pictures of swarming assays were taken a day after spotting. (D) Diameter of swarming colonies measured 24 h after spotting on NB with 5 mM $CaCl_2$. The experiment was performed three times with three replicates per experiment. Diameters of colonies were measured across two locations and averaged. Error bars represent standard deviation between replicates. * denotes a statistically significant difference with a *P* value of $<0.01$ in swarming diameter between the WT and the Δ*cvsS* and Δ*cvsR* strains, determined using Student's two-tailed *t* test. ** denotes a statistically significant difference with a *P* value of $<0.01$ in swarming diameter between the Δ*cvsR* and Δ*cvsR*c strains.

motility (see Fig. S9 in the supplemental material). To see if decreased swarming was due to overproduction of alginate, we compared swarming from a Δ*algD P. syringae* pv. tomato DC3000 strain with that from Δ*cvsS* Δ*algD* and Δ*cvsR* Δ*algD P. syringae* pv. tomato DC3000 strains. Swarming was significantly reduced in the Δ*cvsS* Δ*algD* and Δ*cvsR* Δ*algD P. syringae* pv. tomato DC3000 strains compared to the Δ*algD* strain when grown on swarming medium supplemented with $Ca^{2+}$ (see Fig. S10 in the supplemental material). This suggests that CvsSR regulates swarming motility and possibly biofilm formation when $Ca^{2+}$ is present through a mechanism other than flagellar motility and alginate production.

**CvsSR regulates cellulose production in *P. syringae* pv. tomato DC3000.** *P. syringae* pv. tomato DC3000 has the capability of producing the EPSs Psl, cellulose, and levan along with alginate (5). Psl and cellulose can inhibit swarming in *P. syringae* (45, 46). The genes PSPTO_3529 to PSPTO_3539, which code for proteins that produce Psl, were not differentially expressed between the WT and the Δ*cvsR* strain, nor was there a ChIP-seq peak near these genes. In addition, no difference was found in the amount of Psl between the WT and Δ*cvsS* and Δ*cvsR* strains through the use of a Psl-specific antibody (data not shown) (47), suggesting that the Δ*cvsR* strain and the Δ*cvsS* strain produce the same amount of Psl as the WT. Like the case for Psl, none of the genes that code for the cellulose biosynthetic gene cluster showed differential expression between the Δ*cvsR* strain and the WT in the RNA-Seq data. However, changes in cellulose production can occur even if gene expression for cellulose biosynthesis genes do not show differential expression between two strains, since cellulose is posttranscriptionally

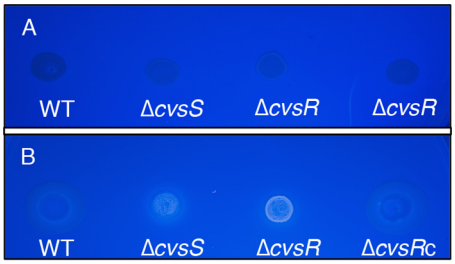


**FIG 5** Growth of the WT, Δ*cvsS*, Δ*cvsR*, and Δ*cvsR*c strains on NB supplemented with 5 mM $CaCl_2$ and CW after 16 h (A) and 3 days (B) of growth. Fluorescence of the bacterial strains under UV light indicates production of cellulose. Bacterial strains were grown to stationary phase in KB medium and resuspended at an $OD_{600}$ of 0.3 in NB medium, and then 5 $\mu$l of each culture was spotted onto the appropriate medium. The plate is representative of assays that were performed three times.

regulated in *P. syringae* pv. tomato DC3000 (48). In order to test for changes in cellulose production, the WT, Δ*cvsS*, Δ*cvsR*, and Δ*cvsR*c strains were grown on NB medium supplemented with $Ca^{2+}$ and calcofluor white (CW). CW is a dye that fluoresces when it binds beta-1,4 glycosyl linkages, and it is commonly used to visualize cellulose production in microbes (48). After 3 days of growth on NB medium supplemented with $Ca^{2+}$ and CW, the Δ*cvsS* and Δ*cvsR* strains fluoresced but the WT and the Δ*cvsR*c strain did not (Fig. 5). In contrast, the WT, Δ*cvsS*, Δ*cvsR*, and Δ*cvsR*c strains did not fluoresce on NB medium supplemented only with CW after 3 days of growth (see Fig. S11 in the supplemental material). From this we conclude that CvsSR regulates cellulose production in *P. syringae* pv. tomato DC3000 when $Ca^{2+}$ is present in the medium.

**CvsSR regulates expression of several T3SS-related genes.** ChIP-seq data showed that *hrpR* and the effectors *hopAT1*, *hopAD1*, *hopAO1*, *avrPtoB*, *hopG1*, *hopD1*, and *hopAA1* had a CvsR binding site upstream of the gene or within the gene itself, suggesting that CvsSR regulates expression of several T3SS genes. A binding site for CvsR was also found upstream of PSPTO_4966, a recently identified member of the HrpL regulon (9). Two recently discovered HrpL-regulated genes, PSPTO_2129 and PSPTO_2130, were the only HrpL-regulated genes differentially expressed between the Δ*cvsR* strain and the WT strain at a fold change cutoff of 2-fold (9, 10). If the fold change cutoff for differentially expressed genes was lowered to 1.7-fold or more, *hopG1* showed increased expression and the pseudogene *hopAT1* showed decreased expression in the Δ*cvsR* strain compared to the WT. Both genes are part of the HrpL regulon. We also observed decreased expression of *hopAH2-1* in the Δ*cvsR* strain compared to the WT. HopAH2-1 is thought to be secreted through the T3SS but is not regulated by HrpL (49). From these data, we conclude that CvsR binds near several T3Es and directly regulates at least two T3Es.

Although differential expression of *hrpRS* was not observed in the RNA-seq data, we investigated whether we could detect differences in expression of *hrpRS* between the Δ*cvsS*, Δ*cvsR*, and WT strains using a reporter gene construct that contained 800 bp upstream of *hrpR* ($P_{hrpRS}$). This reporter gene construct included both CvsR binding sites and should report expression of both *hrpR* and *hrpS* (14). $P_{hrpRS}$ showed a significant decrease in expression in both the Δ*cvsS* and Δ*cvsR* strains compared to the WT when grown in MG medium supplemented with $Ca^{2+}$ but not when grown in MG medium (Fig. 6A; see Fig. S12A in the supplemental material). Since *hrpRS* regulates expression of *hrpL*, it was possible that there was also a difference in *hrpL* expression in the Δ*cvsS* and Δ*cvsR* strains compared to the WT. Therefore, we transformed the WT, Δ*cvsS*, and Δ*cvsR* strains with the vector pBS63, which includes a promoter fusion previously used to measure expression of $P_{hrpL}$ (50). A significant difference in expression of $P_{hrpL}$ in the WT compared to the Δ*cvsS* and Δ*cvsR* strains was seen when strains were grown in MG medium supplemented with $Ca^{2+}$ but not when they were grown in MG medium (Fig. 6B and S12B). Since decreased expression of *hrpRS* and *hrpL* could reduce production of the T3SS and deployment of T3Es, we then tested the hypersensitive response (HR)

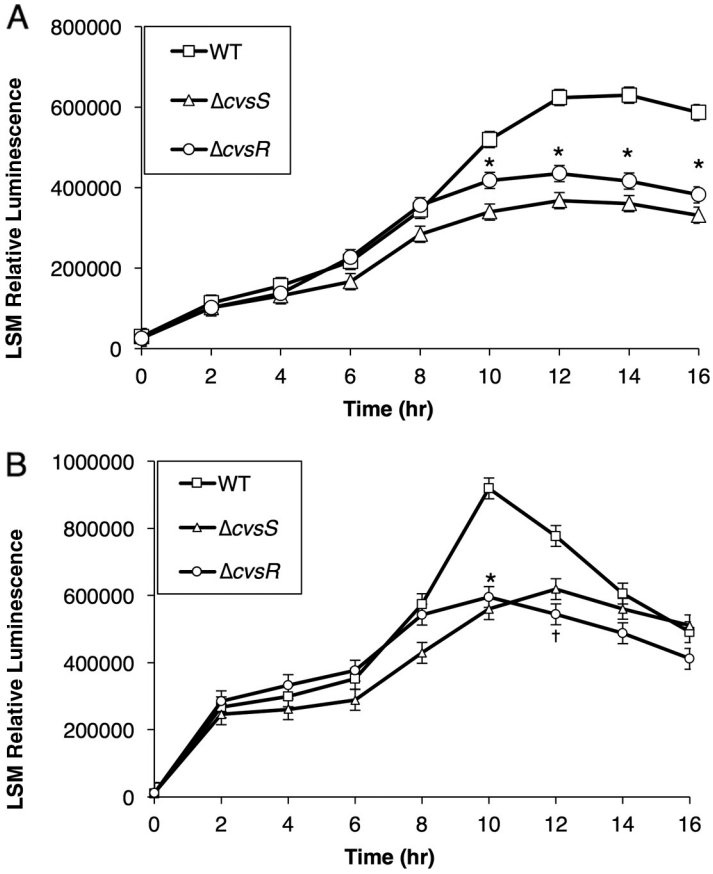


**FIG 6** Luminescence assay to assess activity of $P_{hrpRS}$ (A) and $P_{hrpL}$ (B) in the WT, Δ*cvsS*, and Δ*cvsR* strains when grown in MG supplemented with 5 mM $CaCl_2$. The relative luminescence was calculated using the total luminescence relative to $OD_{600}$. For $P_{hrpRS}$, the experiment was performed three times with three independent replicates per experiment, and for $P_{hrpL}$, the experiment was performed seven times with three independent replicates per experiment. The experiments for each reporter gene construct were compiled using a least-squares mean regression. The error bars represent standard error generated by the differences observed between samples. * denotes statistically significant differences determined using a Tukey HSD test with a *P* value of $<0.01$ between relative luminescence of the WT, Δ*cvsS*, and Δ*cvsR* strains. † denotes statistically significant differences determined using a Tukey HSD test with a *P* value of $<0.01$ between the relative luminescence of the WT and Δ*cvsR* strains.

in *Nicotiana tabacum* and *Nicotiana benthamiana* to see if the Δ*cvsS* and Δ*cvsR* strains would elicit the HR at the same level as the WT. We found no difference in the HR for *N. tabacum* or *N. benthamiana* when infiltrated with the Δ*cvsS* or Δ*cvsR* strain compared to the WT (see Fig. S13 in the supplemental material). Even though CvsSR regulates *hrpRS* and *hrpL*, these data suggest that CvsSR does not affect production of the T3SS or overall deployment of the T3Es during growth *in planta*.

**$Ca^{2+}$ does not influence growth of the Δ*cvsS* and Δ*cvsR* strains *in planta*.** The Δ*cvsR* strain demonstrated increased expression of catalase and genes related to methionine uptake as well as decreased expression of some thiol biosynthesis-related genes (Table 1). Similar gene expression patterns were seen in *Escherichia coli* during treatment with toxic levels of homocysteine and in *E. coli* treated with antimicrobial peptidoglycan recognition proteins (51, 52). This suggests that the bacteria are under distress when grown in a $Ca^{2+}$-supplemented medium. In fact, growth of the Δ*cvsS* and Δ*cvsR* strains was reduced during stationary-phase growth when $Ca^{2+}$ was added to medium (see Fig. S14 in the supplemental material). This concurs with the RNA-seq data and suggests that the Δ*cvsR* strain is under duress when $Ca^{2+}$ is present in media *in vitro*. Since the leaf apoplast is abundant in $Ca^{2+}$, we questioned whether the observed decreases in virulence and growth of the Δ*cvsS* and Δ*cvsR* strains *in planta* are a result

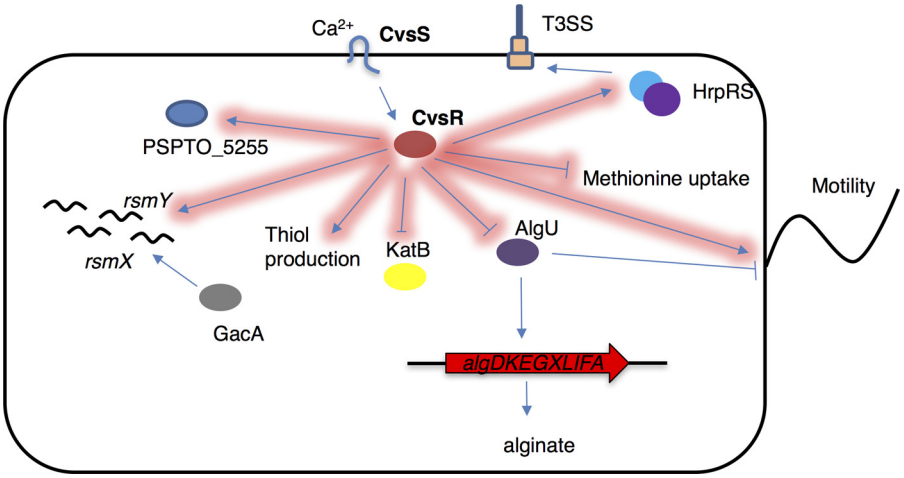


**FIG 7** A partial regulon of CvsR in *P. syringae* pv. tomato DC3000. Arrows highlighted in red are part of the CvsR regulon.

of the concentration of $Ca^{2+}$ in the apoplast. Deleting the T3SS in addition to *cvsS* or *cvsR* should result in an additive loss of growth in tomato leaves if the concentration of $Ca^{2+}$ in the apoplast was the primary cause for the reduced growth of the Δ*cvsS* and Δ*cvsR* strains when inoculated in plants (53). The Δ*hrcQb-U P. syringae* pv. tomato DC3000 strain no longer produces a T3SS and has been used to look at *P. syringae* pv. tomato DC3000-host interactions when it can no longer deliver effectors (54). *P. syringae* pv. tomato DC3000 Δ*hrcQb-U*, Δ*hrcQb-U* Δ*cvsS*, and Δ*hrcQb-U* Δ*cvsR* were syringe infiltrated into tomato leaves. Growth of all of the strains at 4 dpi was similar to that at 6 dpi (see Fig. S15 in the supplemental material). This suggests that the concentration of $Ca^{2+}$ in the apoplast does not adversely affect growth of the Δ*cvsS* and Δ*cvsR* strains.

## DISCUSSION

The results here identify and characterize CvsSR as a virulence-associated TCS that is induced by $Ca^{2+}$ *in vitro* and *in planta*. Through the use of ChIP-seq and RNA-seq, we discovered that CvsSR impacts expression of two main regulators of pathogenicity, *algU* and *hrpRS*. Our results highlight and emphasize the importance of $Ca^{2+}$ as a signal used by *P. syringae* pv. tomato DC3000 during pathogenesis and show that the TCS CvsSR is a key player in the regulation of genes important for full virulence of *P. syringae* pv. tomato DC3000 (Fig. 7).

Mechanisms by which *P. syringae* pv. tomato DC3000 senses and responds to $Ca^{2+}$ were previously unknown. Several TCSs that either sense or are induced by $Ca^{2+}$ have previously been characterized in other bacteria. The histidine kinase PhoQ in *Salmonella enterica* serovar Typhimurium binds to $Ca^{2+}$, $Mg^{2+}$, and $Mn^{2+}$ and regulates several virulence factors (55). CarSR in *Vibrio cholerae* is induced by $Ca^{2+}$ and negatively regulates biofilm formation and exopolysaccharide production (31). In *P. aeruginosa* PAO1, the TCS orthologous to CvsSR, BqsSR, is also induced by $Ca^{2+}$ and regulates the cytosolic $Ca^{2+}$ concentration (38). However, to our knowledge, CvsSR is the first $Ca^{2+}$-induced TCS characterized in a hemibiotrophic plant-pathogenic bacteria. Thus, $Ca^{2+}$ can now be added to the list of environmental cues that *P. syringae* pv. tomato DC3000 uses during pathogenesis.

According to ChIP-seq and RNA-seq data, CvsR directly promotes expression of several genes, including PSPTO_5255, PSPTO_1304, and PSPTO_1609, and directly represses expression of several genes, including *katB* and *tauA* (Table 2). Response regulators within the OmpR family can act as both transcriptional activators and repressors. OmpR in *E. coli* reciprocally regulates *ompF* and *ompC* depending on the osmotic conditions of the environment (56). CpxR in *E. coli* promotes expression of

*marR* and represses expression of *ung* (57, 58). CvsR appears to be similar in its ability to promote and repress expression of different genes.

CvsR regulates transcription of *algU*, and the regulons of CvsR and AlgU have noticeable overlap (15). It is currently unclear how CvsR transcriptionally regulates *algU* in *P. syringae* pv. tomato DC3000. Most characterized negative regulation of *algU* in *Pseudomonas* occurs posttranscriptionally through RsmA or posttranslationally through MucA and MucB (59, 60). Indirect repression of *algU* by CvsR would add another layer of regulatory control over *algU* that was previously unknown. Even with decreased expression of several *rsm* sRNAs and increased expression of *mucA* and *mucB* in the Δ*cvsR* strain compared to the WT, AlgU was still active in the Δ*cvsR* strain (Table 1). One explanation for this phenomenon is that activity of RsmA, MucA, and MucB can be repressed posttranslationally through various mechanisms. Posttranslational repression would not be captured through ChIP-seq or RNA-seq. This could result in reduced activity of these proteins even if there was increased transcription. In the case of MucA, AlgW degrades MucA in *P. aeruginosa*, and something similar could be occurring in the Δ*cvsR* strain (60). For RsmA, *rsmZ* and the *rsmX* paralogs not regulated by CvsR could sequester RsmA in the Δ*cvsR* strain even when the other *rsm* sRNAs are not abundant. Further characterization of CvsR-based *algU* regulation is necessary to discern the exact mechanism.

AlgU regulates expression of genes involved in osmoadaptation, ROS detoxification, alginate biosynthesis, and pathogenicity in *P. syringae* pv. tomato DC3000 (15). Interestingly, and somewhat contradictory to reported results showing that overexpression of *algU* increases virulence of *P. syringae* pv. tomato DC3000, the Δ*cvsR* strain was less virulent than the WT on tomato plants even though it showed an increase in expression of *algU* compared to the WT. Overexpression of *algU* in *P. syringae* pv. tomato DC3000 resulted in increased expression of *cvsS* and *cvsR* (15). Both *cvsS* and *cvsR* are directly regulated by CvsR. Even though we observed upregulation of *algU* in the Δ*cvsR* strain compared to the WT, we did not observe an accompanied upregulation of *cvsS* and *cvsR* in the Δ*cvsR* strain compared to the WT. It is possible that upregulation of *cvsS* and *cvsR* is critically involved in AlgU-related virulence. One might speculate that upon deletion of *cvsR*, *algU* overexpression may no longer positively regulate virulence because upregulation of *cvsSR* no longer occurs.

Biofilm formation and swarming motility are typically antagonistic, with only rare examples of these lifestyles being sympathetic (61). In our study, CvsR appears to regulate biofilm formation and swarming motility in the typical antagonistic way. However, this was not the case with CvsS. The orthologous TCS, BqsSR, in *P. aeruginosa* PAO1 positively regulates biofilm dispersal when *P. aeruginosa* PAO1 is grown in LB (62). However, when grown on BM2 agar supplemented with 10 mM $CaCl_2$, swarming motility was not reduced upon deletion of *bqsSR* (38). As such, while each assay was performed under different conditions, it appears that BqsSR regulates biofilm lifestyle and swarming motility in a sympathetic way in *P. aeruginosa* PAO1. While BqsSR and CvsSR are considered to be orthologous TCSs, they may not function in entirely the same way, and regulation of swarming motility may be an area where these TCSs differ.

Increased EPS production, decreased flagellar motility, and decreased biosurfactant production all result in decreasing swarming motility in *P. syringae* (45, 63). It should be noted that we did not investigate whether changes in biosurfactant production occur in *P. syringae* pv. tomato DC3000 upon deletion of *cvsS* or *cvsR*. However, we did investigate whether changes in EPS production or flagellar motility reduced swarming in the Δ*cvsS* and Δ*cvsR* strains. We ruled out overproduction of alginate as a possible explanation for decreased swarming motility in the Δ*cvsS* and Δ*cvsR* strains (see Fig. S10 in the supplemental material), and there is no clear evidence that the Δ*cvsS* and Δ*cvsR* strains overproduce Psl EPS. It has been reported that increased cellulose production affects swarming motility in *P. syringae* pv. tomato DC3000 (64). We feel that this cannot fully explain the reduced swarming observed in the Δ*cvsS* and Δ*cvsR* strains, since it takes a substantial amount of time to observe noticeable differences in cellulose production in the Δ*cvsS* and Δ*cvsR* strains compared to the WT. Cellulose production

commonly correlates with increased c-di-GMP in *P. syringae* pv. tomato DC3000 (45, 65). Increases in c-di-GMP decrease swarming motility in *Pseudomonas* (66). Although outside the scope of this work, c-di-GMP concentrations in the Δ*cvsR* strain and the WT may differ. Current evidence also suggests that decreased swarming motility is not due to decreased flagellar motility, since swimming is not compromised in the Δ*cvsR* strain. However, the ability to swim is not always reflective of proper flagellar function, as several chemotaxis proteins and flagellar motors are necessary for swarming but not for swimming in *P. aeruginosa* (67, 68). Genes that code for six putative chemotaxis proteins and the rotary flagellar motor protein MotY are downregulated in the Δ*cvsR* strain compared to the WT (Table 1). Therefore, it is possible that downregulation of these genes could reduce swarming without reducing swimming. Further investigation into the role CvsSR plays in swarming is currently being pursued.

CvsR is, to our knowledge, the first direct transcriptional activator of *hrpRS* identified in *P. syringae* pv. tomato DC3000. The conservation of TCSs orthologous to CvsSR in other *P. syringae* pathovars opens the possibility of a conserved *hrpRS* transcriptional activator across pathovars (35). Disruption in *hrpRS* expression in *P. syringae* pv. tomato DC3000 through either deletion of *hrpRS* or deletion of an *hrpRS* indirect regulator, such as GacA, resulted in loss of the HR (14). One curiosity about CvsSR is that deletion of *cvsS* or *cvsR* does not disrupt the HR. Baseline expression of *hrpR* and *hrpS* still occurs when *cvsS* or *cvsR* is deleted. From these data, it is likely that CvsSR tunes expression of *hrpRS*. It is not uncommon for TCSs to tune expression of genes. For example, in *Salmonella enterica*, PhoPQ tunes expression of the effector *steA* during osmotic stress, and PhoBR tunes expression of itself in *E. coli* according to environmental phosphate concentrations (69, 70). If CvsSR tunes expression of *hrpRS*, then it is conceivable that deletion of *cvsS* or *cvsR* may cause only subtle changes T3SS and T3E deployment that do not affect the HR but could still influence pathogenesis.

The exact mechanism by which CvsSR is involved in virulence remains elusive. The growth assay of the Δ*hrcQb-U*, Δ*hrcQb-U* Δ*cvsS*, and Δ*hrcQb-U* Δ*cvsR* strains in tomato brought us to believe that the concentration of $Ca^{2+}$ in the apoplast did not adversely affect growth of the Δ*cvsS* and Δ*cvsR* strains *in planta*. Decreased growth accompanied with decreased virulence of *P. syringae* pv. tomato DC3000, as seen in the Δ*cvsS* and Δ*cvsR* strains when assayed for virulence on tomato plants and *A. thaliana*, could be indicative of increased susceptibility of these strains to the plant immune response or a defect in phytotoxin or T3E deployment in these strains. Decreased spread of chlorotic symptoms by *P. syringae* pv. tomato DC3000 commonly occurs as a result of changes in T3Es or coronatine production (71–73). While we have not investigated whether CvsSR regulates coronatine production in *P. syringae* pv. tomato DC3000, CvsR does bind upstream of several T3Es within the *P. syringae* pv. tomato DC3000 genome. It is possible that regulation of these T3Es by CvsSR *in planta* plays a role in the reduced chlorosis and loss of necrotic specks observed in the plants inoculated with the Δ*cvsS* or the Δ*cvsR* strain. HopAA1-1 is directly regulated by CvsR and is necessary for chlorosis and production of necrotic specks in tomato plants (71). HopG1 is also directly regulated by CvsR and is another T3E that is necessary for chlorosis (74). CvsR also positively regulates expression of the gene *fliC*, which codes for flagellin. Flagellin is a major pathogen-associated molecular pattern (PAMP) that triggers a defense response called PAMP-triggered immunity (PTI) in plants (75). This means that deletion of CvsSR could result in less production of a major PAMP by *P. syringae* pv. tomato DC3000. Decreased expression of PAMPs can recover growth of certain effector-depleted *P. syringae* pv. tomato DC3000 mutants (76). With the regulon of CvsR, including *hrpRS*, several T3Es, and *fliC*, CvsR regulates multiple components involved in virulence of *P. syringae* pv. tomato DC3000. Characterization of the CvsSR regulon *in planta* could provide a clearer picture of how CvsSR regulates each of these factors during endophytic growth and how they synergistically affect virulence of *P. syringae* pv. tomato DC3000.

## MATERIALS AND METHODS

**Bacterial strains and growth conditions.** The primers and bacterial strains and plasmids used in this study are listed in Tables S2 and S3, respectively, in the supplemental material. *Escherichia coli* DH5$\alpha$ and *E. coli* TOP10 (Thermo Fisher Scientific, Waltham, MA) were used for cloning. *E. coli* BL21(DE3) was used for expressing proteins. *E. coli* was grown in Luria-Bertani (LB) medium or Terrific broth (TB) medium supplemented with the appropriate antibiotics when necessary. *P. syringae* pv. tomato DC3000 was routinely cultured on King's B (KB) agar (77). For select assays, strains were grown in MG medium (10 g mannitol, 2.5 g L-glutamate, 0.2 g $MgSO_4 \cdot 7H_2O$, 0.5 g $KH_2PO_4$, and 0.2 g NaCl per liter) at the specified pH (36).

**Creation of *P. syringae* pv. tomato DC3000 mutants.** Unmarked deletion strains were constructed using plasmid pK18mobsacB (78). DNA fragments of approximately 1.1 kb upstream and 1.0 kb downstream of *cvsS* (PSPTO_3380) and *cvsR* (PSPTO_3381) were amplified by PCR, gel purified, and then joined by splicing by overlap extension PCR. These products were then gel purified using a gel extraction miniprep kit (Qiagen, Valencia, CA), digested with the appropriate restriction enzymes, and cloned into pK18mobsacB using EcoRI (New England BioLabs [NEB], Ipswich, MA) and BamHI (NEB). The pK18mobsacB deletion constructs were confirmed by sequencing at the Biotechnology Resource Center of Cornell University before introduction into WT, Δ*hrcQb-U*, or Δ*algD P. syringae* pv. tomato DC3000 via electroporation. Integration events were selected on KB medium containing 50 $\mu$g/ml kanamycin. Colonies were transferred to KB medium containing 10% sucrose to select for crossover events that resulted in the loss of the *sacB* gene. Sucrose-resistant colonies were screened by PCR, and clones containing the appropriate deletion(s) were confirmed by sequencing.

**Complementation of the Δ*cvsR* strain.** The Δ*cvsR* complement was made using a pUC18miniTn*7* vector (79). Briefly a genomic fragment containing *cvsR*, PSPTO_3382, and PSPTO_3383 was amplified via PCR. The products were gel purified using the Qiagen gel extraction miniprep kit (Qiagen), digested with HindIII (NEB) and PstI (NEB), and cloned into a pUC18miniTn*7* plasmid which had been digested with HindIII and PstI. The resulting ligation was transformed into DH5$\alpha$ *E. coli* cells. The Δ*cvsR P. syringae* pv. tomato DC3000 strain was transformed through electroporation with pUC18miniTn*7*::*cvsR*-3383 and the helper plasmid pTNS2. Colonies were selected by plating on KB supplemented with 10 $\mu$g/ml gentamicin. Positive clones were confirmed through sequencing.

**Creation of a CvsR-FLAG-tagged strain.** The CvsR-FLAG-tagged strain was made using pBS46 (80). Briefly, the sequence for a FLAG tag was added to the 3′ end of *cvsR* (*cvsR*-FLAG) using PCR amplification. The PCR product was gel extracted using the Zymoclean gel extraction kit (Zymo, Irvine, CA) and then cloned into a pENTR/SD/TOPO vector (Thermo Fisher Scientific) and transformed into Top10 *E. coli* (Thermo Fisher Scientific). Positive clones for pENTR/SD/TOPO::*cvsR*-FLAG were selected by plating on LB supplemented with 50 $\mu$g/ml kanamycin agar plates and confirmed through sequencing. *cvsR*-FLAG was moved to from the pENTR/SD/TOPO entry vector to a vector containing an *nptII* promoter, pBS46, using the LR reaction (Thermo Fisher Scientific) and transformed into TOP10 *E. coli* (Thermo Fisher Scientific). Positive clones were selected on LB agar plates supplemented with 10 $\mu$g/ml gentamicin and confirmed through sequencing. Δ*cvsR P. syringae* pv. tomato DC3000 was then transformed with pBS46::*cvsR*-FLAG and selected on KB agar plates supplemented with 10 $\mu$g/ml gentamicin.

**Luciferase reporter assays.** Four hundred base pairs upstream of PSPTO_3383 ($P_{cvsSR}$) and 850 bp upstream of *hrpR* ($P_{hrpRS}$) were PCR amplified. The PCR products were purified using a Qiagen PCR purification kit (Qiagen), cloned into pENTR/D/TOPO vectors (Thermo Fisher Scientific), and transformed into TOP10 *E. coli* (Thermo Fisher Scientific). Positive clones and constructs for pENTR/D/TOPO::p3383 and pENTR/D/TOPO::p*hrpR* were generated, selected, and transformed into appropriate strains of *P. syringae* pv. tomato DC3000 as previously described (81).

*P. syringae* pv. tomato DC3000 strains were grown on KB plates and transferred to MG medium (pH 6.0) or apoplastic washing fluid (AWF) at an optical density at 600 nm ($OD_{600}$) of 0.1; 5 mM $CaCl_2$ or 5 mM EGTA was added to the cultures when appropriate. Strains were grown in 96-well plates (Nunc) at 28°C with shaking in a Biotek Synergy II microplate reader (Winooski, VT). $OD_{600}$ and luminescence measurements were taken every 2 h. Relative luminescence measurements were normalized to $OD_{600}$. The assays were repeated three times, and sampling was conducted in triplicate. Averages and standard deviations were generated from each experiment. Statistical significance was determined by performing a least-squares mean regression on the combined biological replicates.

**Extraction of AWF.** A procedure used to extract apoplastic washing fluid (AWF) from bean plants was used to extract AWF on 3- to 4-week-old *Solanum lycopersicum* cv. Moneymaker plants (82). After extracting AWF, samples were analyzed for cellular contamination by testing for glucose-6-phosphate dehydrogenase and maltose dehydrogenase activity using a glucose-6-phosphate dehydrogenase activity assay kit (Sigma) and a maltose dehydrogenase activity assay kit (Sigma). AWF was then lyophilized and resuspended to an equivalent undiluted state.

**ICP-MS.** AWF was diluted 4-fold and 80-fold, depending on the element being examined, in double-deionized water ($ddH_2O$) and analyzed on an iCap Q inductively coupled plasma mass spectrometer (ICP-MS) (Thermo Fisher Scientific). Standards for calcium, potassium, zinc, sulfur, iron, cadmium, magnesium, and phosphorus (Thermo Fisher Scientific) were included for each sample tested.

**Tomato virulence assays.** Three- to 4-week old *Solanum lycopersicum* cv. Moneymaker plants were inoculated with the WT, Δ*cvsS*, Δ*cvsR*, and Δ*cvsR*c *P. syringae* pv. tomato DC3000 strains at $2 \times 10^7$ CFU/ml through dip inoculation as was previously described (83). To assay the Δ*hrcQb-U*, Δ*hrcQb-U* Δ*cvsS*, and Δ*hrcQb-U* Δ*cvsR* strains, 3- to 4-week-old *Solanum lycopersicum* cv. Moneymaker plants were inoculated with *P. syringae* pv. tomato DC3000 strains at $1 \times 10^6$ CFU/ml using a blunt-tipped syringe. Time points for growth of the bacteria (in CFU/mg) were 4 and 6 days postinoculation (dpi). The

experiment was repeated three times, and three technical replicates were performed for each experiment. Averages and standard deviations were generated for growth of bacteria for each experiment. Student's two-tailed *t* test was used to determine statistical significance between growth of different strains.

***A. thaliana* virulence assays.** *A. thaliana* was grown and inoculated as previously described (84). Plants were dipped in a bacterial suspension at $3 \times 10^4$ CFU/ml and vacuum infiltrated at 20 mm Hg. Symptoms were observed at 4 and 6 dpi, and growth of the bacteria (CFU/mg) was measured at 4 and 6 dpi. The experiment was repeated three times, and three replicates were used during each experiment. Averages and standard deviations were generated for growth of bacteria for each experiment.

**HR assays.** Three- to 4-week-old *N. tabacum* cv. xanthi or *N. benthamiana* plants were syringe infiltrated with *P. syringae* pv. tomato DC3000 strains resuspended in 10 mM $MgCl_2$ at $2 \times 10^6$, $2 \times 10^7$, and $2 \times 10^8$ CFU/ml (85). The hypersensitive response (HR) was observed 1 and 2 dpi. Pictures were taken at 2 dpi. This experiment was repeated three times with three technical replicates for each biological replicate.

**ChIP and preparation of DNA for ChIP-seq.** The Δ*cvsR P. syringae* pv. tomato DC3000 strain complemented with pBS46::*cvsR*-FLAG was grown overnight in KB medium to stationary phase, and 200 μl of the culture was plated on NB (Becton Dickinson, Franklin Lake, NJ) medium supplemented with 5 mM $CaCl_2$ and 0.5% (wt/vol) sodium succinate hexahydrate (Sigma). After 18 h of growth at 28°C, the cells were scraped from the plates using a sterile slide, resuspended in NB medium with 1% formaldehyde, and then processed as described previously (37).

**qPCR.** Quantitative PCR (qPCR) was performed on DNA from input and IP fractions on a CFX Connect (Bio-Rad, Hercules, CA) using Sso Advanced SYBR green Supermix (Bio-Rad). Primers upstream of PSPTO_3383 were used to determine enrichment for predicted targets of CvsR in the IP fraction. Enrichment of these areas was determined relative to regions in the gene *gyrA* (37).

**Analysis of ChIP-seq data.** Sequenced reads from three separate MiSeq runs were first compiled and then analyzed. Sequencing reads were trimmed using the FASTX toolkit (version 0.0.14) and the UTILS toolkit (release tag 822) (86). Bowtie2 2.2.6 was used to align sequencing reads to the *P. syringae* pv. tomato DC3000 genome (87). Ambiguous reads were removed using a custom script as previously described (88). MACS version 2.1.0.20140616 was used to identify regions of enrichment in the *P. syringae* pv. tomato DC3000 genome from the IP sample using the following parameters: macs2 callpeak −t CHIP_FILE −c CONTROL_FILE, −seed 1 −g 6.1e6 −fix-bimodal\, and −keep-dup all −q 0.0.5. Several peaks were called within *cvsR*. Since these were likely artifacts due to overexpression of *cvsR* during the ChIP-seq experiment, they were disregarded.

**CvsR binding motif generation.** Regions 50 bp up- and downstream of called peaks were identified. Any regions that overlapped were merged. These regions were then compiled, and motif discovery was performed using MEME version 4.10.0 patchlevel 1 with the following parameters (89): −revcomp −nmotifs 3 −minw 6 −maxw 50\, −minsites 2 −maxsites NUMBER_OF_INPUT_SEQUENCES, and −mod zoops.

**RNA extraction and RNA-seq cDNA library preparation.** *P. syringae* pv. tomato DC3000 strains were grown overnight in KB medium to stationary phase, and 200 μl of these cultures was plated and spread on NB medium with 5 mM $CaCl_2$ supplemented with 0.5% (wt/vol) sodium succinate hexahydrate. The cultures were allowed to grow for 18 h at 28°C, and then RNA was extracted using the Direct-zol kit (Zymo). rRNA was then extracted using Ribo-zero for Gram-negative bacteria (Illumina, Madison, WI) as previously described (88). cDNA libraries were made using Scriptseq V.2 according to the manufacturer's instructions. The cDNA libraries were sequenced on a HiSeq 2000 at the Cornell Core Facility.

**Analysis of RNA-seq data.** Sequenced reads were first trimmed using fastq-mcf (release tag 1.04.807) and then aligned to the *P. syringae* pv. tomato DC3000 genome using Bowtie2 2.2.6 (87). Ambiguous reads were removed as previously described (88). Next, a list of regions to be considered for differential analysis was constructed as previously described (15).

**qRT-PCR.** Extracted RNA was reverse transcribed into cDNA using the qScript cDNA Supermix (Quanta, Gaithersburg, MD). Quantitative reverse transcription-PCR (qRT-PCR) was performed on a Bio-Rad CFX Connect using Sso Advanced SYBR green Supermix. The reference gene *gyrA* was used to normalize expression between samples (90). Experiments were performed three times. Averages and standard deviations from each biological replicate were generated from the experiments.

**RT-PCR.** Extracted RNA was reverse transcribed into cDNA using the iScript cDNA Supermix (Bio-Rad). In addition, a control with no reverse transcriptase was made using extracted RNA as well. RT-PCR was performed on *P. syringae* pv. tomato DC3000 genomic DNA, cDNA, and an RNA control without reverse transcriptase on a Bio-Rad T100 thermocycler using OneTaq (NEB). PCR products were then run on an agar gel and visualized using a ChemiDoc transilluminator (Bio-Rad). RT-PCR experiments were performed three times on three biological replicates.

**Overproduction and purification of CvsR.** The *cvsR* gene was amplified with Phusion (Thermo Fisher Scientific) using primers oMRF0355 and oMRF0356 and *P. syringae* pv. tomato DC3000 genomic DNA as a template. Amplified *cvsR* was cloned into pET21 using NotI and SpeI (NEB) to make pET21::*cvsR* (pMRF21). pMRF21 was transformed into BL21(DE3) *E. coli* cells (Thermo Fisher Scientific). Transformed cells were grown at 37°C in 4 liters of LB medium supplemented with 100 μg/ml ampicillin to an $OD_{600}$ of 0.8 before 0.5 mM IPTG (isopropyl-β-D-thiogalactopyranoside) (Sigma) was added to the culture to induce expression. Cells were allowed to grow for another 4 h at 37°C and then pelleted and frozen at −80°C. Thawed cells were resuspended in wash buffer (20 mM Tris [pH 8], 500 mM KCl, 20 mM imidazole, and 10% glycerol) and lysed through sonication. Insoluble material was removed through centrifugation,

and the supernatant was applied to Ni-nitrilotriacetic acid (Ni-NTA) Superflow agarose (Qiagen) using gravity column chromatography. CvsR was eluted off the agarose using elution buffer (20 mM Tris [pH 8], 500 mM KCl, 100 mM imidazole, and 10% glycerol), dialyzed overnight into storage buffer (40.1 mM $K_2HPO_4$, 9.9 mM $KH_2PO_4$ [pH 7.4], 300 mM KCl, 50% glycerol), and stored at −80°C.

**EMSA.** 6-Carboxyfluorescein (6-FAM)-labeled probes were generated through PCR with OneTaq (NEB) using *P. syringae* pv. tomato DC3000 genomic DNA as a template. Probes were gel purified using the Zymoclean gel DNA recovery kit (Zymo). Electrophoretic mobility shift assays (EMSA) were performed with increasing concentrations of CvsR (0 nM to 500 nM). Labeled probes were incubated with CvsR in 20 $\mu$l of binding buffer [40.1 mM $K_2HPO_4$, 9.9 mM $KH_2PO_4$ (pH 7.4), 15 mM KCl, 1 mM $MgSO_4$, 10% glycerol, and 40 ng/$\mu$l poly(dI-dC) DNA (Thermo Fisher)] for 20 min at room temperature. The reaction mixtures were then added to 6% polyacrylamide gels (0.5× Tris-borate-EDTA [TBE], 29:1 acrylamide-bisacrylamide [Bio-Rad], 30% glycerol) and run at 215 V for 3 h on ice. Gels were visualized on a Typhoon 9400 image system (GE Healthcare, Pittsburgh, PA).

**Nonradioactive DNase footprinting.** 6-FAM-labeled probes were generated and purified in the same manner as for EMSA. DNase footprinting assays were performed with 1 to 4 $\mu$M CvsR. Labeled probes were incubated with CvsR in 20 $\mu$l of DNase footprinting buffer (15 mM Tris-HCl [pH 7.4], 10 mM KCl, 6 mM $MgSO_4$, 1 mM $CaCl_2$, 10% glycerol, 2.5 ng/$\mu$l salmon sperm DNA [Sigma], 100 $\mu$g/ml bovine serum albumin [NEB]) for 20 min at room temperature, and then 0.001 U of DNase (NEB) was added to reaction mixtures and allowed to incubate for 2 min before a volume of DNase stop solution (20 mM EDTA [pH 8.0], 1% SDS, 200 mM NaCl) equal to that of the reaction mixture was added. Digested probes were purified using the Oligo Clean and Concentrator (Zymo). Results were analyzed as previously described (37). The locations of regions protected by CvsR were estimated by mapping the position of the binding site back to the genomic location of the probe using a LIZ500 ladder (Thermo Fisher Scientific). The genomic locations of regions protected by CvsR were compiled, and motif discovery was performed on MEME version 4.11.3 (89) with the following parameters (89): −revcomp −nmotifs 3 −minw 4 −maxw 50 −mod zoops\.

**Quantification of alginate.** *P. syringae* pv. tomato DC3000 strains were grown overnight in KB medium to stationary phase, and 200 $\mu$l of these cultures was plated and spread on NB agar or NB agar supplemented with 5 mM $CaCl_2$ plates. The cultures were grown at 28°C before being scraped off the plate and resuspended in 0.9% NaCl. Resuspended cells were pelleted by centrifugation, supernatant was removed, and alginate production was determined using the carbazole-borate method with sodium alginate (Sigma-Aldrich) as a standard (91).

**Motility assays.** Swarming assays were performed using NB plates containing 0.5% (wt/vol) agar supplemented with 5 mM $CaCl_2$ when appropriate. *P. syringae* pv. tomato DC3000 strains were grown overnight in KB medium, and 5 $\mu$l of each culture was spotted on a swarming plate (92). Swarming zones were measured after plates were incubated for 24 h at room temperature. Student's two-tailed *t* test was used to determine statistical significance.

Swimming assays were performed using swimming plates (10 g tryptone, 5 g NaCl per liter) with 0.3% (wt/vol) agar and supplemented with 5 mM $CaCl_2$ when appropriate (93). *P. syringae* pv. tomato DC3000 strains were grown overnight in KB medium. Toothpicks were dipped into the overnight cultures grown to stationary phase in KB medium and inserted into the centers of the swimming plates (94). Diameters of bacterial zones were measured after plates were incubated for 48 h. Pictures of swimming zones were taken after 24 h of growth at room temperature.

**Biofilm assays.** Biofilm assays were modified from a previously described protocol (95). *P. syringae* pv. tomato DC3000 strains were grown overnight at 28°C in KB medium, washed twice with MG medium, and then subinoculated into MG medium (pH 7.0) with 2 mM $CaCl_2$ at an $OD_{600}$ of 0.02. One hundred microliters of each bacterial suspension was grown in clear flat-bottom 96-well plates in a BioTek Synergy 2 microplate reader for 24 h at 28°C with shaking. Cultures were removed from the wells using a pipette, and then the wells were washed with double-distilled $H_2O$ ($ddH_2O$). Following washing, wells were stained with 0.1% crystal violet for 10 min and washed twice with $ddH_2O$. Stained biofilms were dissolved with 100 $\mu$l of 30% acetic acid, and the $OD_{570}$ was recorded using a Biotek Synergy 2 microplate reader. Experiments were repeated three times. Four technical replicates of each strain were used during each experiment. Student's two-tailed *t* test was used to determine statistical significance.

**Statistical analysis.** All statistical analysis was performed using JMP Pro 12.

## SUPPLEMENTAL MATERIAL

Supplemental material for this article may be found at https://doi.org/10.1128/JB.00538-17.

**SUPPLEMENTAL FILE 1,** PDF file, 0.6 MB.

**SUPPLEMENTAL FILE 2,** XLSX file, 0.1 MB.

## ACKNOWLEDGMENTS

We thank Kent Loeffler and Claire Smith for pictures used in this article. We thank Eric Craft and Shree K. Giri for running samples for ICP-MS. We thank Alan Collmer for reviewing the manuscript and providing helpful comments.

Mention of trade names or commercial products in this publication is solely for the

purposes of providing specific information and does not imply recommendation or endorsement by the USDA.

We declare no conflicts of interest.

## REFERENCES


1. Hirano SS, Upper CD. 1990. Population biology and epidemiology of *Pseudomonas syringae*. Annu Rev Phytopathol 28:155–177. https://doi.org/10.1146/annurev.py.28.090190.001103.
2. Baltrus DA, Nishimura MT, Romanchuk A, Chang JH, Mukhtar MS, Cherkis K, Roach J, Grant SR, Jones CD, Dangl JL. 2011. Dynamic evolution of pathogenicity revealed by sequencing and comparative genomics of 19 *Pseudomonas syringae* isolates. PLoS Pathog 7:e1002132. https://doi.org/10.1371/journal.ppat.1002132.
3. Green S, Laue B, Fossdal CG, A'Hara SW, Cottrell JE. 2009. Infection of horse chestnut (*Aesculus hippocastanum*) by *Pseudomonas syringae pv. aesculi* and its detection by quantitative real-time PCR. Plant Pathol 58:731–744. https://doi.org/10.1111/j.1365-3059.2009.02065.x.
4. McCann HC, Rikkerink EHA, Bertels F, Fiers M, Lu A, Rees-George J, Andersen MT, Gleave AP, Haubold B, Wohlers MW, Guttman DS, Wang PW, Straub C, Vanneste J, Rainey PB, Templeton MD. 2013. Genomic analysis of the kiwifruit pathogen *Pseudomonas syringae* pv. *actinidiae* provides insight into the origins of an emergent plant disease. PLoS Pathog 9:e1003503. https://doi.org/10.1371/journal.ppat.1003503.
5. Buell CR, Joardar V, Lindeberg M, Selengut J, Paulsen IT, Gwinn ML, Dodson RJ, Deboy RT, Durkin AS, Kolonay JF, Madupu R, Daugherty S, Brinkac L, Beanan MJ, Haft DH, Nelson WC, Davidsen T, Zafar N, Zhou L, Liu J, Yuan Q, Khouri H, Fedorova N, Tran B, Russell D, Berry K, Utterback T, Van Aken SE, Feldblyum TV, D'Ascenzo M, Deng W-L, Ramos AR, Alfano JR, Cartinhour S, Chatterjee AK, Delaney TP, Lazarowitz SG, Martin GB, Schneider DJ, Tang X, Bender CL, White O, Fraser CM, Collmer A. 2003. The complete genome sequence of the *Arabidopsis* and tomato pathogen *Pseudomonas syringae pv. tomato* DC3000. Proc Natl Acad Sci U S A 100:10181–10186. https://doi.org/10.1073/pnas.1731982100.
6. Gill US, Lee S, Mysore KS. 2015. Host versus nonhost resistance: distinct wars with similar arsenals. Phytopathology 105:580–587. https://doi.org/10.1094/PHYTO-11-14-0298-RVW.
7. Xin XF, He SY. 2013. *Pseudomonas syringae pv. tomato* DC3000: a model pathogen for probing disease susceptibility and hormone signaling in plants. Annu Rev Phytopathol 51:473–498. https://doi.org/10.1146/annurev-phyto-082712-102321.
8. Lindeberg M, Stavrinides J, Chang JH, Alfano JR, Collmer A, Dangl JL, Greenberg JT, Mansfield JW, Guttman DS. 2005. Proposed guidelines for a unified nomenclature and phylogenetic analysis of type III Hop effector proteins in the plant pathogen *Pseudomonas syringae*. Mol Plant Microbe Interact 18:275–282. https://doi.org/10.1094/MPMI-18-0275.
9. Lam HN, Chakravarthy S, Wei H-L, BuiNguyen H, Stodghill PV, Collmer A, Swingle BM, Cartinhour SW. 2014. Global analysis of the HrpL regulon in the plant pathogen *Pseudomonas syringae pv. tomato* DC3000 reveals new regulon members with diverse functions. PLoS One 9:e106115. https://doi.org/10.1371/journal.pone.0106115.
10. Ferreira AO, Myers CR, Gordon JS, Martin GB, Vencato M, Collmer A, Wehling MD, Alfano JR, Moreno-Hagelsieb G, Lamboy WF, DeClerck G, Schneider DJ, Cartinhour SW. 2006. Whole-genome expression profiling defines the HrpL regulon of *Pseudomonas syringae pv. tomato* DC3000, allows de novo reconstruction of the Hrp cis clement, and identifies novel coregulated genes. Mol Plant Microbe Interact 19:1167–1179. https://doi.org/10.1094/MPMI-19-1167.
11. Jovanovic M, James EH, Burrows PC, Rego FGM, Buck M, Schumacher J. 2011. Regulation of the co-evolved HrpR and HrpS AAA+ proteins required for *Pseudomonas syringae* pathogenicity. Nat Commun 2:177. https://doi.org/10.1038/ncomms1177.
12. Lan L, Deng X, Zhou J, Tang X. 2006. Genome-wide gene expression analysis of *Pseudomonas syringae* pv. *tomato DC3000* reveals overlapping and distinct pathways regulated by *hrpL* and *hrpRS*. Mol Plant Microbe Interact 19:976–987. https://doi.org/10.1094/MPMI-19-0976.
13. Deng X, Liang H, Chen K, He C, Lan L, Tang X. 2014. Molecular mechanisms of two-component system RhpRS regulating type III secretion system in *Pseudomonas syringae*. Nucleic Acids Res 42:11472–11486. https://doi.org/10.1093/nar/gku865.
14. Chatterjee A, Cui Y, Yang H, Collmer A, Alfano JR, Chatterjee AK. 2003. GacA, the response regulator of a two-component system, acts as a master regulator in *Pseudomonas syringae pv. tomato* DC3000 by controlling regulatory RNA, transcriptional activators, and alternate sigma factors. Mol Plant Microbe Interact 16:1106–1117. https://doi.org/10.1094/MPMI.2003.16.12.1106.
15. Markel E, Stodghill P, Bao Z, Myers CR, Swingle B. 2016. AlgU controls expression of virulence genes in *Pseudomonas syringae pv. tomato* DC3000. J Bacteriol 198:2330–2344. https://doi.org/10.1128/JB.00276-16.
16. Moll S, Schneider DJ, Stodghill P, Myers CR, Cartinhour SW, Filiatrault MJ. 2010. Construction of an *rsmX* co-variance model and identification of five *rsmX* non-coding RNAs in *Pseudomonas syringae pv. tomato* DC3000. RNA Biol 7:508–516. https://doi.org/10.4161/rna.7.5.12687.
17. Kong HS, Roberts DP, Patterson CD, Kuehne SA, Heeb S, Lakshman DK, Lydon J. 2012. Effect of overexpressing rsmA from *Pseudomonas aeruginosa* on virulence of select phytotoxin-producing strains of *P. syringae*. Phytopathology 102:575–587. https://doi.org/10.1094/PHYTO-09-11-0267.
18. Hershberger CD, Ye RW, Parsek MR, Xie ZD, Chakrabarty AM. 1995. The *algT* (*algU*) gene of *Pseudomonas aeruginosa*, a key regulator involved in alginate biosynthesis, encodes an alternative sigma factor (sigma E). Proc Natl Acad Sci U S A 92:7941–7945. https://doi.org/10.1073/pnas.92.17.7941.
19. Stael S, Wurzinger B, Mair A, Mehlmer N, Vothknecht UC, Teige M. 2012. Plant organellar calcium signalling: an emerging field. J Exp Bot 63:1525–1542. https://doi.org/10.1093/jxb/err394.
20. O'Leary BM, Neale HC, Geilfus C-M, Jackson RW, Arnold DL, Preston GM. 2016. Early changes in apoplast composition associated with defence and disease in interactions between *Phaseolus vulgaris* and the halo blight pathogen *Pseudomonas syringae* pv. *phaseolicola*. Plant Cell Environ 39:2172–2184. https://doi.org/10.1111/pce.12770.
21. De La Fuente L, Parker JK, Oliver JE, Granger S, Brannen PM, van Santen E, Cobine PA. 2013. The bacterial pathogen *Xylella fastidiosa* affects the leaf ionome of plant hosts during infection. PLoS One 8:e62945. https://doi.org/10.1371/journal.pone.0062945.
22. Dominguez DC, Guragain M, Patrauchan M. 2015. Calcium binding proteins and calcium signaling in prokaryotes. Cell Calcium 57:151–165. https://doi.org/10.1016/j.ceca.2014.12.006.
23. Norris V, Chen M, Goldberg M, Voskuil J, McGurk G, Holland B. 1991. Calcium in bacteria: a solution to which problem? Mol Microbiol 5:775–778. https://doi.org/10.1111/j.1365-2958.1991.tb00748.x.
24. Dominguez DC. 2004. Calcium signalling in bacteria. Mol Microbiol 54:291–297. https://doi.org/10.1111/j.1365-2958.2004.04276.x.
25. Werthen M, Lundgren T. 2001. Intracellular Ca(2+) mobilization and kinase activity during acylated homoserine lactone-dependent quorum sensing in *Serratia liquefaciens*. J Biol Chem 276:6468–6472. https://doi.org/10.1074/jbc.M009223200.
26. Guragain M, Lenaburg DL, Moore FS, Reutlinger I, Patrauchan MA. 2013. Calcium homeostasis in *Pseudomonas aeruginosa* requires multiple transporters and modulates swarming motility. Cell Calcium 54:350–361. https://doi.org/10.1016/j.ceca.2013.08.004.
27. Gode-Potratz CJ, Chodur DM, McCarter LL. 2010. Calcium and iron regulate swarming and type III secretion in *Vibrio parahaemolyticus*. J Bacteriol 192:6025–6038. https://doi.org/10.1128/JB.00654-10.
28. Cruz LF, Cobine PA, De La Fuente L. 2012. Calcium increases *Xylella fastidiosa* surface attachment, biofilm formation, and twitching motility. Appl Environ Microbiol 78:1321–1331. https://doi.org/10.1128/AEM.06501-11.
29. Sarkisova S, Patrauchan MA, Berglund D, Nivens DE, Franklin MJ. 2005. Calcium-induced virulence factors associated with the extracellular matrix of mucoid *Pseudomonas aeruginosa* biofilms. J Bacteriol 187:4327–4337. https://doi.org/10.1128/JB.187.13.4327-4337.2005.
30. Patrauchan MA, Sarkisova S, Sauer K, Franklin MJ. 2005. Calcium influences cellular and extracellular product formation during biofilm-associated growth of a marine *Pseudoalteromonas* sp. Microbiology 151:2885–2897. https://doi.org/10.1099/mic.0.28041-0.
31. Bilecen K, Yildiz FH. 2009. Identification of a calcium-controlled negative regulatory system affecting *Vibrio cholerae* biofilm formation. Environ Microbiol 11:2015–2029. https://doi.org/10.1111/j.1462-2920.2009.01923.x.
32. Parker JK, Chen H, McCarty SE, Liu LY, De La Fuente L. 2016. Calcium

transcriptionally regulates the biofilm machinery of *Xylella fastidiosa* to promote continued biofilm development in batch cultures. Environ Microbiol 18:1620–1634. https://doi.org/10.1111/1462-2920.13242.
33. Flego D, Pirhonen M, Saarilahti H, Palva TK, Palva ET. 1997. Control of virulence gene expression by plant calcium in the phytopathogen *Erwinia carotovora*. Mol Microbiol 25:831–838. https://doi.org/10.1111/j.1365-2958.1997.mmi501.x.
34. Stock AM, Robinson VL, Goudreau PN. 2000. Two-component signal transduction. Annu Rev Biochem 69:183–215. https://doi.org/10.1146/annurev.biochem.69.1.183.
35. Lavin JL, Kiil K, Resano O, Ussery DW, Oguiza JA. 2007. Comparative genomic analysis of two-component regulatory proteins in *Pseudomonas syringae*. BMC Genomics 8:397. https://doi.org/10.1186/1471-2164-8-397.
36. Bronstein PA, Filiatrault MJ, Myers CR, Rutzke M, Schneider DJ, Cartinhour SW. 2008. Global transcriptional responses of *Pseudomonas syringae* DC3000 to changes in iron bioavailability in vitro. BMC Microbiol 8:209. https://doi.org/10.1186/1471-2180-8-209.
37. Butcher BG, Bronstein PA, Myers CR, Stodghill PV, Bolton JJ, Markel EJ, Filiatrault MJ, Swingle B, Gaballa A, Helmann JD, Schneider DJ, Cartinhour SW. 2011. Characterization of the Fur regulon in *Pseudomonas syringae pv. tomato* DC3000. J Bacteriol 193:4598–4611. https://doi.org/10.1128/JB.00340-11.
38. Guragain M, King MM, Williamson KS, Perez-Osorio AC, Akiyama T, Khanam S, Patrauchan MA, Franklin MJ. 2016. The *Pseudomonas aeruginosa* PAO1 two-component regulator CarSR regulates calcium homeostasis and calcium-induced virulence factor production through its regulatory targets CarO and CarP. J Bacteriol 198:951–963. https://doi.org/10.1128/JB.00963-15.
39. Filiatrault MJ, Stodghill PV, Myers CR, Bronstein PA, Butcher BG, Lam H, Grills G, Schweitzer P, Wang W, Schneider DJ, Cartinhour SW. 2011. Genome-wide identification of transcriptional start sites in the plant pathogen *Pseudomonas syringae pv. tomato* str DC3000. PLoS One 6:e29335. https://doi.org/10.1371/journal.pone.0029335.
40. Kreamer NN, Wilks JC, Marlow JJ, Coleman ML, Newman DK. 2012. BqsR/BqsS constitute a two-component system that senses extracellular Fe(II) in *Pseudomonas aeruginosa*. J Bacteriol 194:1195–1204. https://doi.org/10.1128/JB.05634-11.
41. Perkins TT, Davies MR, Klemm EJ, Rowley G, Wileman T, James K, Keane T, Maskell D, Hinton JCD, Dougan G, Kingsley RA. 2013. ChIP-seq and transcriptome analysis of the OmpR regulon of *Salmonella enterica* serovars *Typhi* and *Typhimurium* reveals accessory genes implicated in host colonization. Mol Microbiol 87:526–538. https://doi.org/10.1111/mmi.12111.
42. Hay ID, Remminghorst U, Rehm BH. 2009. MucR, a novel membrane-associated regulator of alginate biosynthesis in *Pseudomonas aeruginosa*. Appl Environ Microbiol 75:1110–1120. https://doi.org/10.1128/AEM.02416-08.
43. Kaplan JB. 2010. Biofilm dispersal: mechanisms, clinical implications, and potential therapeutic uses. J Dent Res 89:205–218. https://doi.org/10.1177/0022034509359403.
44. Daniels R, Vanderleyden J, Michiels J. 2004. Quorum sensing and swarming migration in bacteria. FEMS Microbiol Rev 28:261–289. https://doi.org/10.1016/j.femsre.2003.09.004.
45. Pérez-Mendoza D, Aragón IM, Prada-Ramírez HA, Romero-Jiménez L, Ramos C, Gallegos M-T, Sanjuán J. 2014. Responses to elevated c-di-GMP levels in mutualistic and pathogenic plant-interacting bacteria. PLoS One 9:e91645. https://doi.org/10.1371/journal.pone.0091645.
46. Records AR, Gross DC. 2010. Sensor kinases RetS and LadS regulate *Pseudomonas syringae* type VI secretion and virulence factors. J Bacteriol 192:3584–3596. https://doi.org/10.1128/JB.00114-10.
47. Byrd MS, Sadovskaya I, Vinogradov E, Lu H, Sprinkle AB, Richardson SH, Ma L, Ralston B, Parsek MR, Anderson EM, Lam JS, Wozniak DJ. 2009. Genetic and biochemical analyses of the *Pseudomonas aeruginosa* Psl exopolysaccharide reveal overlapping roles for polysaccharide synthesis enzymes in Psl and LPS production. Mol Microbiol 73:622–638. https://doi.org/10.1111/j.1365-2958.2009.06795.x.
48. Ude S, Arnold DL, Moon CD, Timms-Wilson T, Spiers AJ. 2006. Biofilm formation and cellulose expression among diverse environmental *Pseudomonas* isolates. Environ Microbiol 8:1997–2011. https://doi.org/10.1111/j.1462-2920.2006.01080.x.
49. Vinatzer BA, Jelenska J, Greenberg JT. 2005. Bioinformatics correctly identifies many type III secretion substrates in the plant pathogen *Pseudomonas syringae* and the biocontrol isolate *P. fluorescens* SBW25. Mol Plant Microbe Interact 18:877–888. https://doi.org/10.1094/MPMI-18-0877.
50. McCraw SL, Park DH, Jones R, Bentley MA, Rico A, Ratcliffe RG, Kruger NJ, Collmer A, Preston GM. 2016. GABA (γ-aminobutyric acid) uptake via the GABA permease GabP represses virulence gene expression in *Pseudomonas syringae pv. tomato* DC3000. Mol Plant Microbe Interact 29:938–949. https://doi.org/10.1094/MPMI-08-16-0172-R.
51. Fraser KR, Tuite NL, Bhagwat A, O'Byrne CP. 2006. Global effects of homocysteine on transcription in *Escherichia coli*: induction of the gene for the major cold-shock protein, CspA. Microbiology 152:2221–2231. https://doi.org/10.1099/mic.0.28804-0.
52. Kashyap DR, Rompca A, Gaballa A, Helmann JD, Chan J, Chang CJ, Hozo I, Gupta D, Dziarski R. 2014. Peptidoglycan recognition proteins kill bacteria by inducing oxidative, thiol, and metal stress. PLoS Pathog 10:e1004280. https://doi.org/10.1371/journal.ppat.1004280.
53. Ortiz-Martín I, Thwaites R, Macho AP, Mansfield JW, Beuzón CR. 2010. Positive regulation of the Hrp Type III secretion system in *Pseudomonas syringae* pv. *phaseolicola*. Mol Plant Microbe Interact 23:665–681. https://doi.org/10.1094/MPMI-23-5-0665.
54. Badel JL, Shimizu R, Oh H-S, Collmer A. 2006. A *Pseudomonas syringae* pv. tomato *avrE1/hopM1* mutant is severely reduced in growth and lesion formation in tomato. Mol Plant Microbe Interact 19:99–111. https://doi.org/10.1094/MPMI-19-0099.
55. Prost LR, Miller SI. 2008. The *Salmonellae* PhoQ sensor: mechanisms of detection of phagosome signals. Cell Microbiol 10:576–582. https://doi.org/10.1111/j.1462-5822.2007.01111.x.
56. Yoshida T, Qin L, Egger LA, Inouye M. 2006. Transcription regulation of *ompF* and *ompC* by a single transcription factor, OmpR. J Biol Chem 281:17114–17123. https://doi.org/10.1074/jbc.M602112200.
57. Ogasawara H, Teramoto J, Hirao K, Yamamoto K, Ishihama A, Utsumi R. 2004. Negative regulation of DNA repair gene (*ung*) expression by the CpxR/CpxA two-component system in *Escherichia coli* K-12 and induction of mutations by increased expression of CpxR. J Bacteriol 186:8317–8325. https://doi.org/10.1128/JB.186.24.8317-8325.2004.
58. Weatherspoon-Griffin N, Yang D, Kong W, Hua Z, Shi Y. 2014. The CpxR/CpxA two-component regulatory system up-regulates the multidrug resistance cascade to facilitate *Escherichia coli* resistance to a model antimicrobial peptide. J Biol Chem 289:32571–32582. https://doi.org/10.1074/jbc.M114.565762.
59. Martínez-Granero F, Navazo A, Barahona E, Redondo-Nieto M, Rivilla R, Martín M. 2012. The Gac-Rsm and SadB signal transduction pathways converge on AlgU to downregulate motility in *Pseudomonas fluorescens*. PLoS One 7:e31765. https://doi.org/10.1371/journal.pone.0031765.
60. Wood LF, Ohman DE. 2009. Use of cell wall stress to characterize σ22 (AlgT/U) activation by regulated proteolysis and its regulon in *Pseudomonas aeruginosa*. Mol Microbiol 72:183–201. https://doi.org/10.1111/j.1365-2958.2009.06635.x.
61. Verstraeten N, Braeken K, Debkumari B, Fauvart M, Fransaer J, Vermant J, Michiels J. 2008. Living on a surface: swarming and biofilm formation. Trends Microbiol 16:496–506. https://doi.org/10.1016/j.tim.2008.07.004.
62. Dong YH, Zhang XF, An SW, Xu JL, Zhang LH. 2008. A novel two-component system BqsS-BqsR modulates quorum sensing-dependent biofilm decay in *Pseudomonas aeruginosa*. Commun Integr Biol 1:88–96. https://doi.org/10.4161/cib.1.1.6717.
63. Burch AY, Shimada BK, Mullin SW, Dunlap CA, Bowman MJ, Lindow SE. 2012. *Pseudomonas syringae* coordinates production of a motility-enabling surfactant with flagellar assembly. J Bacteriol 194:1287–1298. https://doi.org/10.1128/JB.06058-11.
64. Zorraquino V, Garcia B, Latasa C, Echeverz M, Toledo-Arana A, Valle J, Lasa I, Solano C. 2013. Coordinated cyclic-di-GMP repression of *Salmonella* motility through YcgR and cellulose. J Bacteriol 195:417–428. https://doi.org/10.1128/JB.01789-12.
65. Prada-Ramirez HA, Perez-Mendoza D, Felipe A, Martinez-Granero F, Rivilla R, Sanjuan J, Gallegos MT. 2016. AmrZ regulates cellulose production in *Pseudomonas syringae pv. tomato* DC3000. Mol Microbiol 99:960–977. https://doi.org/10.1111/mmi.13278.
66. Kuchma SL, Delalez NJ, Filkins LM, Snavely EA, Armitage JP, O'Toole GA. 2015. Cyclic di-GMP-mediated repression of swarming motility by *Pseudomonas aeruginosa* PA14 requires the MotAB stator. J Bacteriol 197:420–430. https://doi.org/10.1128/JB.02130-14.
67. Toutain CM, Zegans ME, O'Toole GA. 2005. Evidence for two flagellar stators and their role in the motility of *Pseudomonas aeruginosa*. J Bacteriol 187:771–777. https://doi.org/10.1128/JB.187.2.771-777.2005.
68. Terashima H, Kojima S, Homma M. 2008. Flagellar motility in bacteria. Int

Rev Cell Mol Biol 270:39–85. https://doi.org/10.1016/S1937-6448(08)01402-0.
69. Cardenal-Muñoz E, Ramos-Morales F. 2013. DsbA and MgrB regulate *steA* expression through the two-component system PhoQ/PhoP in *Salmonella enterica*. J Bacteriol 195:2368–2378. https://doi.org/10.1128/JB.00110-13.
70. Gao R, Stock AM. 2013. Evolutionary tuning of protein expression levels of a positively autoregulated two-component system. PLoS Genet 9:e1003927. https://doi.org/10.1371/journal.pgen.1003927.
71. Munkvold KR, Russell AB, Kvitko BH, Collmer A. 2009. *Pseudomonas syringae pv. tomato* DC3000 type III effector HopAA1-1 functions redundantly with chlorosis-promoting factor PSPTO4723 to produce bacterial speck lesions in host tomato. Mol Plant Microbe Interact 22:1341–1355. https://doi.org/10.1094/MPMI-22-11-1341.
72. Worley JN, Russell AB, Wexler AG, Bronstein PA, Kvitko BH, Krasnoff SB, Munkvold KR, Swingle B, Gibson DM, Collmer A. 2013. *Pseudomonas syringae pv. tomato* DC3000 CmaL (PSPTO4723), a DUF1330 family member, is needed to produce L-allo-isoleucine, a precursor for the phytotoxin coronatine. J Bacteriol 195:287–296. https://doi.org/10.1128/JB.01352-12.
73. Chakravarthy S, Worley JN, Montes-Rodriguez A, Collmer A. 2017. *Pseudomonas syringae* pv. *tomato* DC3000 polymutants deploying coronatine and two type III effectors produce quantifiable chlorotic spots from individual bacterial colonies in *Nicotiana benthamiana* leaves. Mol Plant Pathol https://doi.org/10.1111/mpp.12579.
74. Guo M, Kim P, Li G, Elowsky Christian G, Alfano James R. 2016. A bacterial effector co-opts calmodulin to target the plant microtubule network. Cell Host Microbe 19:67–78. https://doi.org/10.1016/j.chom.2015.12.007.
75. Felix G, Duran JD, Volko S, Boller T. 1999. Plants have a sensitive perception system for the most conserved domain of bacterial flagellin. Plant J 18:265–276. https://doi.org/10.1046/j.1365-313X.1999.00265.x.
76. Kvitko BH, Park DH, Velásquez AC, Wei C-F, Russell AB, Martin GB, Schneider DJ, Collmer A. 2009. Deletions in the repertoire of *Pseudomonas syringae* pv. *tomato* DC3000 type III secretion effector genes reveal functional overlap among effectors. PLoS Pathog 5:e1000388. https://doi.org/10.1371/journal.ppat.1000388.
77. King EO, Ward MK, Raney DE. 1954. Two simple media for the demonstration of pyocyanin and fluorescin. J Lab Clin Med 44:301–307.
78. Schafer A, Tauch A, Jager W, Kalinowski J, Thierbach G, Puhler A. 1994. Small mobilizable multi-purpose cloning vectors derived from the *Escherichia coli* plasmids pK18 and pK19: selection of defined deletions in the chromosome of *Corynebacterium glutamicum*. Gene 145:69–73. https://doi.org/10.1016/0378-1119(94)90324-7.
79. Choi KH, Schweizer HP. 2006. Mini-Tn7 insertion in bacteria with single attTn7 sites: example *Pseudomonas aeruginosa*. Nat Protoc 1:153–161. https://doi.org/10.1038/nprot.2006.24.
80. Swingle B, Thete D, Moll M, Myers CR, Schneider DJ, Cartinhour S. 2008. Characterization of the PvdS-regulated promoter motif in *Pseudomonas syringae pv. tomato* DC3000 reveals regulon members and insights regarding PvdS function in other pseudomonads. Mol Microbiol 68:871–889. https://doi.org/10.1111/j.1365-2958.2008.06209.x.
81. Markel E, Maciak C, Butcher BG, Myers CR, Stodghill P, Bao Z, Cartinhour S, Swingle B. 2011. An extracytoplasmic function sigma factor-mediated cell surface signaling system in *Pseudomonas syringae pv. tomato* DC3000 regulates gene expression in response to heterologous siderophores. J Bacteriol 193:5775–5783. https://doi.org/10.1128/JB.05114-11.
82. O'Leary BM, Rico A, McCraw S, Fones HN, Preston GM. 2014. The infiltration-centrifugation technique for extraction of apoplastic fluid from plant leaves using *Phaseolus vulgaris* as an example. J Vis Exp https://doi.org/10.3791/52113.
83. Park SH, Butcher BG, Anderson Z, Pellegrini N, Bao Z, D'Amico K, Filiatrault MJ. 2013. Analysis of the small RNA P16/RgsA in the plant pathogen *Pseudomonas syringae pv. tomato* strain DC3000. Microbiology 159:296–306. https://doi.org/10.1099/mic.0.063826-0.
84. Wei CF, Kvitko BH, Shimizu R, Crabill E, Alfano JR, Lin NC, Martin GB, Huang HC, Collmer A. 2007. A *Pseudomonas syringae* pv. *tomato* DC3000 mutant lacking the type III effector HopQ1-1 is able to cause disease in the model plant *Nicotiana benthamiana*. Plant J 51:32–46. https://doi.org/10.1111/j.1365-313X.2007.03126.x.
85. Lelliott RA, Billing E, Hayward AC. 1966. A determinative scheme for the fluorescent plant pathogenic pseudomonads. J Appl Bacteriol 29:470–489. https://doi.org/10.1111/j.1365-2672.1966.tb03499.x.
86. Aronesty E. 2013. Comparison of sequencing utility programs. Open Bioinform J 7:1–8. https://doi.org/10.2174/1875036201307010001.
87. Langmead B, Salzberg SL. 2012. Fast gapped-read alignment with Bowtie 2. Nat Methods 9:357–359. https://doi.org/10.1038/nmeth.1923.
88. Filiatrault MJ, Stodghill PV, Bronstein PA, Moll S, Lindeberg M, Grills G, Schweitzer P, Wang W, Schroth GP, Luo S, Khrebtukova I, Yang Y, Thannhauser T, Butcher BG, Cartinhour S, Schneider DJ. 2010. Transcriptome analysis of *Pseudomonas syringae* identifies new genes, noncoding RNAs, and antisense activity. J Bacteriol 192:2359–2372. https://doi.org/10.1128/JB.01445-09.
89. Bailey TL, Boden M, Buske FA, Frith M, Grant CE, Clementi L, Ren J, Li WW, Noble WS. 2009. MEME Suite: tools for motif discovery and searching. Nucleic Acids Res 37:W202–W208. https://doi.org/10.1093/nar/gkp335.
90. Vencato M, Tian F, Alfano JR, Buell CR, Cartinhour S, DeClerck GA, Guttman DS, Stavrinides J, Joardar V, Lindeberg M, Bronstein PA, Mansfield JW, Myers CR, Collmer A, Schneider DJ. 2006. Bioinformatics-enabled identification of the HrpL regulon and type III secretion system effector proteins of *Pseudomonas syringae pv. phaseolicola* 1448A. Mol Plant Microbe Interact 19:1193–1206. https://doi.org/10.1094/MPMI-19-1193.
91. Knutson CA, Jeanes A. 1968. A new modification of the carbazole analysis: application to heteropolysaccharides. Anal Biochem 24:470–481. https://doi.org/10.1016/0003-2697(68)90154-1.
92. Deziel E, Lepine F, Milot S, Villemur R. 2003. *rhlA* is required for the production of a novel biosurfactant promoting swarming motility in *Pseudomonas aeruginosa*: 3-(3-hydroxyalkanoyloxy)alkanoic acids (HAAs), the precursors of rhamnolipids. Microbiology 149:2005–2013. https://doi.org/10.1099/mic.0.26154-0.
93. Rashid MH, Kornberg A. 2000. Inorganic polyphosphate is needed for swimming, swarming, and twitching motilities of *Pseudomonas aeruginosa*. Proc Natl Acad Sci U S A 97:4885–4890. https://doi.org/10.1073/pnas.060030097.
94. Tremblay J, Richardson AP, Lepine F, Deziel E. 2007. Self-produced extracellular stimuli modulate the *Pseudomonas aeruginosa* swarming motility behaviour. Environ Microbiol 9:2622–2630. https://doi.org/10.1111/j.1462-2920.2007.01396.x.
95. Merritt JH, Kadouri DE, O'Toole GA. 2005. Growing and analyzing static biofilms. Curr Protoc Microbiol Chapter 1:Unit 1B 1.
96. Finn RD, Attwood TK, Babbitt PC, Bateman A, Bork P, Bridge AJ, Chang H-Y, Dosztányi Z, El-Gebali S, Fraser M, Gough J, Haft D, Holliday GL, Huang H, Huang X, Letunic I, Lopez R, Lu S, Marchler-Bauer A, Mi H, Mistry J, Natale DA, Necci M, Nuka G, Orengo CA, Park Y, Pesseat S, Piovesan D, Potter SC, Rawlings ND, Redaschi N, Richardson L, Rivoire C, Sangrador-Vegas A, Sigrist C, Sillitoe I, Smithers B, Squizzato S, Sutton G, Thanki N, Thomas PD, Tosatto Silvio CE, Wu CH, Xenarios I, Yeh L-S, Young S-Y, Mitchell AL. 2017. InterPro in 2017—beyond protein family and domain annotations. Nucleic Acids Res 45:D190–D199. https://doi.org/10.1093/nar/gkw1107.
97. Uniprot Consortium. 2017. UniProt: the universal protein knowledgebase. Nucleic Acids Res 45:D158–D169. https://doi.org/10.1093/nar/gkw1099.